Pergamon

J. Mech. Phys. Solids, Vol. 45, No. 8, pp. 1357–1392, 1997

0022–5096/97 $17.00+0.00

PII: S0022–5096(96)00118–4

NONLINEAR BEHAVIOR OF WAVY COMPOSITES UNDER TENSION

A. CHISKIS, R. PARNES AND L. SLEPYAN

Department of Solid Mechanics, Materials and Structures, Faculty of Engineering, Tel-Aviv University, Ramat Aviv 69978, Israel

(*Received* 17 *April* 1996; *in revised form* 28 *October* 1996)

ABSTRACT

A composite structure consisting of doubly periodic moderately wavy layers under tension is considered. The periodic cell of the composite is represented by two layers of different materials, but having the same arbitrary initial shape. As opposed to theories with full homogenization, the thickness of the periodic cell with respect to its length is not assumed to approach zero in the analysis. The influence of this structural parameter is shown to be especially significant if the material of one of the layers is much weaker than the other.

Using a geometrical nonlinear Cosserat rod model to describe the layers, we take into account extension, flexure and shear deformation in the layers. The problem is reduced to a boundary value problem for a scalar nonlinear ODE of second order for the rotational degree of freedom. The determination of the deformed shape of the layers, as well as the relation between the elongation of the periodic cell and the applied tension force is then reduced to nonlinear quadratures. For the case of small initial waviness, an analytical solution is obtained for an arbitrary initial shape of the layers. For moderate initial waviness, numerical results are presented relating stress, strain and amplitude of waviness. The influence of material and structural parameters is investigated and discussed. © 1997 Elsevier Science Ltd

Keywords: A. microstructures, B. layered material, B. finite deflections, B. Cosserat continuum.

1. INTRODUCTION

We investigate the problem of uni-axial extension of a plane doubly periodic structure consisting of curvilinear elastic layers with periods $2L$ and H in the X- and Y-directions, respectively (see Fig. 1). Here H is the thickness of the double layer packet which consists of two layers of different thicknesses and material properties but having the same arbitrary initial shape.

Wavy composites have attracted great attention in recent times. Such composites can possess significant nonlinear properties [see Luo and Chou (1990)]. Because of the geometrical nonlinearity, they fall within the class of materials having a high level of strain energy under extension [see Cherkaev and Slepyan (1995)]. In particular, we note that these nonlinear features can be especially important in dynamics where even an inextensible layer can accumulate energy.

Historically, the investigation of plane finite deformations of fiber-reinforced materials originated with studies of incompressible constrained materials [see Adkins

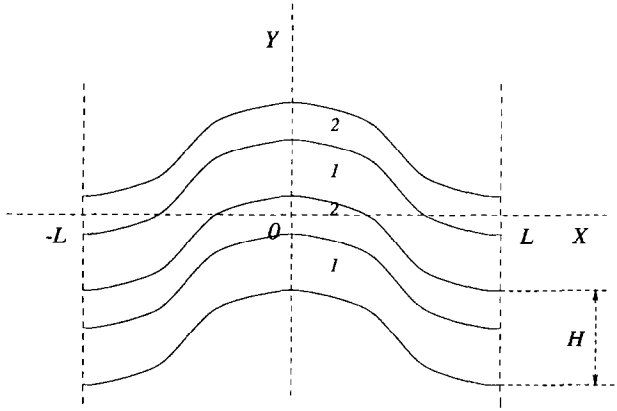

Fig. 1. Wavy composite in the initial configuration. The periodic cell is represented by the double layer packet with constant Y-thickness H and $X \in [-L, L]$.

(1956), Pipkin (1977), Pipkin and Rogers (1971) and Spencer (1972)]. The composite material was treated as a homogeneous continuum under constraints imposed by curvilinear fibers (or cords). The first articles modeling the nonlinear behavior of wavy composites where the material properties of the matrix as well as of the fibers are taken into account and where no hypothesis of fiber inextensibility is made, appear to be those of Chou and Takahashi (1987) and later Luo and Chou (1988, 1990). These articles are based on laminate theory where, as a main assumption, the segments of material are assumed to behave as straight composite laminae (with specified properties, obtained experimentally). However, having different orientations, the laminae then have different responses to a given stress field. By adding the deformations of the pieces contained in an X-period of the wavy composite, one then obtains the "macro" strain. Another approach is based on a homogenization asymptotic technique of singular perturbation for PDEs with highly oscillating coefficients. Such a treatment of the *linear* problem in the framework of linear elasticity was represented by Skoller and Hegemier (1995).

A significant aspect of the behavior of wavy composites is the influence of the H/L structural parameter. Physically, this influence corresponds to taking into account the flexural rigidity of the layers. We note that this parameter does not appear in any straight-laminate based theory where only volume concentrations are present [see Chou and Takahashi (1987) and Luo and Chou (1988, 1990)]. In the singular perturbation asymptotic technique [as in Skoller and Hegemier (1995)] this parameter is also absent in the standard first term approximation of the asymptotic series.

With the purpose of formulating the corresponding theory of such a composite we use here a nonlinear Cosserat rod model to describe the layers. Application of linear classical rod theories to wavy composites is not new, [for example, Feltman and Santare (1994), in their study of the forming of thermoplastic composites with wavy fibres, used linearized beam-column theory with an additional simplification that the fibers are inextensible]. However, the application of the nonlinear Cosserat rod theory to wavy composites, as far as we know, has not been considered. In this present study,

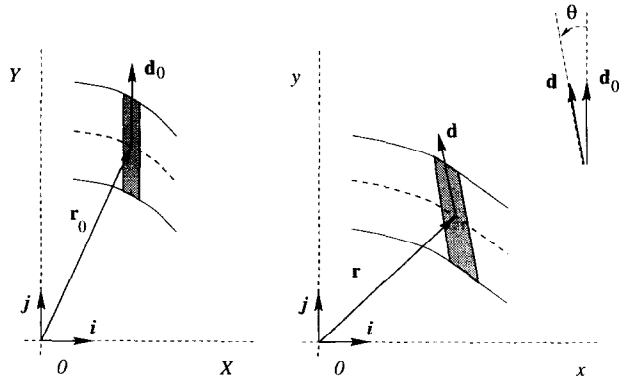

Fig. 2. Deformation of Cosserat layer. The shaded areas represent material elements in the initial configuration (with radius vector $\mathbf{r}_0$ and orientation $\mathbf{d}_0$) and in the deformed configuration (with radius vector $\mathbf{r}$ and orientation $\mathbf{d}$)

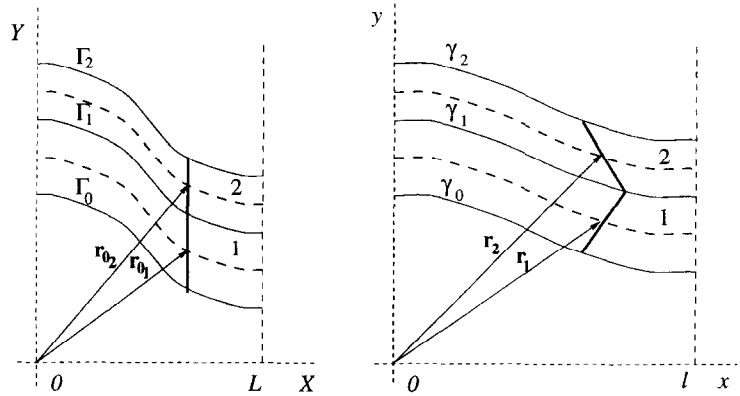

Fig. 3. Deformation of the double layer packet. Solid line represents the common cross-section in the initial configuration and rotated cross-sections of the two layers in the deformed configuration. The two segments of the material elements belonging to the two layers rotate through angles θ_1 and θ_2, respectively. Due to Y-periodicity, the upper and the lower ends of the cross-section have the same x-coordinate.

each layer is represented by its reference curve described by a position vector in the deformed configuration and by the rotation of the cross-section attached to the reference curve (see Fig. 2). Hence, in the X–Y plane, three independent degrees of freedom exist for the cross-section element of any layer of the packet: two translational and one rotational. The deformation of the double layer packet is shown in Fig. 3. Thus this Cosserat model takes into account extension, flexure and shear deformation in the layers. The importance of taking shear into account immediately follows from the waviness and periodicity of the considered structure, as shown in Fig. 3. Note that in the case when one layer is much stiffer than the other, the deviation between the tangent vector and the normal vector to the deformed cross-section can be significant in the weak layer.

Using the layer interface continuity conditions as well as the periodicity conditions, we write relations between the radius vectors of the layers and between the angles of rotation of each layer, as well as the relation between distributed forces in the layers (which are due to the interface traction forces). We then show that the entire packet can be described as a one-dimensional continuum governed by the three independent degrees of freedom mentioned above. The equilibrium equations corresponding to the translational degrees of freedom can be easily integrated, resulting in a relation independent of the specific constitutive equations of the layers. The third degree of freedom, related to rotations, is represented by an auxiliary angle from which the angles of rotation of each of the layers of the cross-section can be determined. An approximate relation for the distributed moments in the layers is proposed; using this relation, we write the basic equation for the rotational degree of freedom. It is worth noting that the present model is valid for the full range of material properties of the layers; for example, in two possible extremal cases: if one layer material is much weaker than the other, the packet behaves as a single curvilinear layer consisting only of the stiff layer; if the materials of the layers are the same, the analytic expression and the results are seen, within the accuracy of the theory, to degenerate to a description of a homogeneous continuum.

The problem is finally reduced to a boundary value problem for a scalar nonlinear ODE of second order for the above mentioned auxiliary angle. The calculation of the angles of rotation, calculated via this angle, is significantly simplified if the parameter H/L is small. In this case the ODE becomes singular and we show that the auxiliary angle is determined (asymptotically) as a solution of a transcendental equation. The determination of the deformed shape of the layers as well as the relation between the elongation of the periodic cell and the applied tension force is then reduced to nonlinear quadratures.

An analytical solution of the problem for the case of small, but arbitrary, initial waviness is also presented. Numerical results of the problem under a prescribed moderate initial waviness are given for different relations of the Young modulus of the layers and various values of the H/L structural parameter. A qualitative analysis of the results is presented.

For small values of H/L, the resulting stress–strain curves given by Chou and Takahashi (1987) are in good agreement with our results. However, we show that, as expected, for increasing values of the parameter H/L, the flexural behavior assumes greater importance and the overall behavior changes significantly, particularly if the material properties of the layers differ strongly.

We mention here a restriction imposed by the proposed model, namely that neither the shear nor the elongation of the materials can be too large. This large shear can possibly arise if the stiffnesses of the layers differ greatly under a low volume concentration of the weak layer. In this case we would observe a large shear in this layer leading to a large deviation between the tangent vector and the cross-section in the layer. As a result, the geometrically nonlinear—but physically linear—model would not be valid. Note that in the opposite case, which is of more practical importance, i.e. when the volume concentration of the stiff layer material is small, this effect does not appear and the model is appropriate.

While the investigation is in the framework of a geometrically nonlinear Cosserat

model using linear constitutive equations, the approach is, however, quite general and is equally valid for nonlinear constitutive equations.

2. FORMULATION OF THE PROBLEM

2.1. *The initial geometry and boundary conditions*

We consider an infinite composite material composed of a slightly curvilinear ("wavy") double layer structure (Fig. 1) which undergoes extension in the X-direction. In the initial configuration each layer has the same period $2L$ in the X-direction and the set of two layers is periodic with period H in the Y-direction. We shall refer to each layer as the α-layer ($\alpha = 1, 2$), and to the set of the two layers as the *double layer packet* or, more briefly, as the *packet*. The cross-sections of each α-layer, lying perpendicular to the X-axis are assumed to have a constant thickness in the Y-direction, H_α, such that the thickness H of the packet is

$$H = H_1 + H_2. \tag{2.1}$$

Layers in the packet differ by their material properties and by layer thicknesses. Assuming the packet to be slender ($H \ll 2L$) we shall apply rod theory to each layer.

In this model, the interfaces between the layers in the initial configuration are specified to have the same shape,

$$Y = Y_0(X), \quad Y_0(X) = Y_0(X+2L), \tag{2.2}$$

where $Y_0(X)$ is a given function expressed in Lagrangian coordinates. This function therefore represents a *template* curve which, when shifted in the Y-direction, defines the interfaces.

We assume further that $Y_0(X)$ is an even function with zero slope at $X = 0$ and $X = L$, i.e.

$$Y_0(X) = Y_0(-X), \quad \frac{\mathrm{d}Y_0(0)}{\mathrm{d}X} = \frac{\mathrm{d}Y_0(L)}{\mathrm{d}X} = 0. \tag{2.3}$$

By virtue of the periodicity in X, and the properties (2.3), a solution to the problem can be obtained by investigating a given *cell*, $0 \leqslant X \leqslant L$, $-\infty \leqslant Y \leqslant \infty$.

Due to application of a tension force to the material in the X-direction, the material undergoes deformation with displacements in the X- and Y- directions. We denote the position vector at any point in the deformed configuration by $\mathbf{x} = x\mathbf{i} + y\mathbf{j}$.

Corresponding to the applied extension and periodicity of the structure, we impose the following boundary conditions (Fig. 2):

i. $$x(0, Y) = 0, \quad x(L, Y) = l, \tag{2.4}$$

where $2l$ is the period of the deformed cell.

ii. The shear stress along the lines $x = 0$ and $x = l$ (corresponding to $X = 0$ and $X = L$) vanish. (We observe that this condition is consistent with (2.3).)

We further assume that:

iii. The surface of the corresponding real body (at "large" $|Y|$) is traction free. For the periodical structure considered, it follows that the corresponding forces are zero, i.e. $\int_0^l \sigma_{yy} dx = \int_0^l \sigma_{yx} dx = 0$.

In addition to determining the average traction along the line $X = L$ as a function of the imposed extension, $\bar{\varepsilon} = (l/L) - 1$, the material parameter and the geometrical parameters, we wish to determine the shape of the deformed packet.

2.2. *Kinematical hypotheses*

In this section we introduce several kinematical hypotheses which allow us to create a rather simple model of the wavy composite, also taking into account the bending rigidity of the layers. Specifically:

(1) We assume, as in common rod/shell theories, that the deformation of the layer cross-section is plane (hypothesis 1).
(2) We assume that the midlines of the layers deform identically (hypothesis 2). This leads to significant simplification of the model; this hypothesis seems to describe the true picture of the deformation rather well. Note that such an assumption is implicitly made in any theory based on a laminate approach.
(3) We do not determine the thickness of the *deformed* layers but assume that the thickness ratio is invariable in the process of deformation and is equal to the volume fraction ratio (hypothesis 3); this hypothesis leads to a relation between angles of rotation of the layers.

The above hypotheses, as well as the force hypothesis 4, lead to a consistent phenomenological model of the wavy composite.

We represent each two-dimensional layer as a rod described by the position vector $\mathbf{r}$ in the deformed configuration (and $\mathbf{r}_0$ in the initial configuration) to its *reference curve* and by a rotation of the "body-particle" attached to the reference curve (Fig. 2). The body-particle has (in the X–Y plane) three *independent* degrees of freedom: two translational and one rotational. The rotational degree of freedom can be described by the rotation of the *director*, $\mathbf{d}$:

$$\mathbf{d} = \mathbf{P}(\theta)\mathbf{d}_0, \tag{2.5}$$

where

$$\mathbf{P}(\theta) = \begin{pmatrix} \cos\theta & -\sin\theta \\ \sin\theta & \cos\theta \end{pmatrix}$$

is the plane rotational tensor, θ is the angle of rotation, and where $\mathbf{d}_0$ and $\mathbf{d}$, representing the director in the initial and in the deformed configurations, respectively, are each unit vectors attached to the body-particle as shown in Fig. 2. This model, representing the simplest (nonlinear) model which takes flexure, axial extension and shear into account, is a Cosserat model [see Antman (1972, 1994) and Eliseev (1988)].

In considering the kinematical interface condition, we adopt the usual assumption, namely **(kinematical) hypothesis 1**: cross-sections of each α-layer remain plane and rotate through an angle θ_α ($\alpha = 1, 2$), as defined by the attached directors $\mathbf{d}_\alpha$.

Noting that the initial shape of all the reference curves is the same, we choose the *middle* curve of a layer as its reference curve. We further choose the initial arc length S along the template curve (2.2),

$$S = \int_0^X (1 + (\mathrm{d}Y_0/\mathrm{d}X)^2)^{1/2} \mathrm{d}X \tag{2.6}$$

as the Lagrangian coordinate for all the layers; thus we write $\mathbf{r}_{0\alpha} = \mathbf{r}_{0\alpha}(S)$, $\mathbf{d}_{0\alpha} = \mathbf{d}_{0\alpha}(S)$, $\mathbf{r}_\alpha = \mathbf{r}_\alpha(S)$, $\mathbf{d}_\alpha = \mathbf{d}_\alpha(S)$ and $\theta_\alpha = \theta_\alpha(S)$ where $\alpha = 1, 2$ for the double layer packet (Fig. 3). Note that the intersection of a given line $X = const.$ with the interface curves (Γ_0, Γ_1 and Γ_2) and with the reference curve corresponds to the same value S along these lines (Fig. 3). In particular, $X = 0$ and $X = L$ correspond to $S = 0$ and S_L, where the value S_L can be calculated by (2.6).

The initial tangent vector is then the same for both layer curves in the packet, i.e.

$$\mathbf{r}_{01}' = \mathbf{r}_{02}' = \mathbf{t}_0, \tag{2.7}$$

where $(\ldots)'$ denotes $\mathrm{d}(\ldots)/\mathrm{d}S$, and where $\mathbf{t}_0$ is the tangent vector to the initial layer reference curve.

It is convenient to *choose*

$$\mathbf{d}_{0\alpha} = \mathbf{j} \quad (\alpha = 1, 2) \tag{2.8}$$

for *all* body points in *both* layers. Then due to (2.5) we have

$$\mathbf{d}_\alpha = -\sin\theta_\alpha \mathbf{i} + \cos\theta_\alpha \mathbf{j}. \tag{2.9}$$

We note that the director, (2.8), associated with the cross-section, is *not* orthogonal to the initial tangent vector; it lies in cross-sections which initially are cut by lines $X = const.$

Upon deformation of the packet, the initial interface curves Γ_k ($k = 0, 1, 2$) map to the deformed interface curves γ_k ($k = 0, 1, 2$) (Fig. 3). However, due to the periodicity, the boundaries of the packet γ_0 and γ_2, must necessarily have the same shape. Furthermore, due to the Y-periodicity on the packet interface, points (lying on Γ_0, Γ_2) which have the same X-coordinates in the initial configuration have the same x-coordinates in the deformed configuration (Fig. 3). This leads us to **(kinematical) hypothesis 2**:

$$\mathbf{r}_1'(S) = \mathbf{r}_2'(S) \equiv \mathbf{r}'(S), \tag{2.10}$$

namely all reference curves deform identically.

By virtue of the *periodicity* and the *displacement continuity* condition at the inner interface line, γ_1, we have (Fig. 4)

$$h_1 \tan\theta_1 + h_2 \tan\theta_2 = 0, \tag{2.11}$$

where h_α ($\alpha = 1, 2$) are the projections of the *rotated* cross-sections in the y-direction. We observe that the angles θ_1 and θ_2 have different sign and that the values h_1 and h_2 are unknown.

In the present investigation, we need not determine h_1 and h_2 but we instead assume, as an approximation, namely **(kinematical) hypothesis 3**:

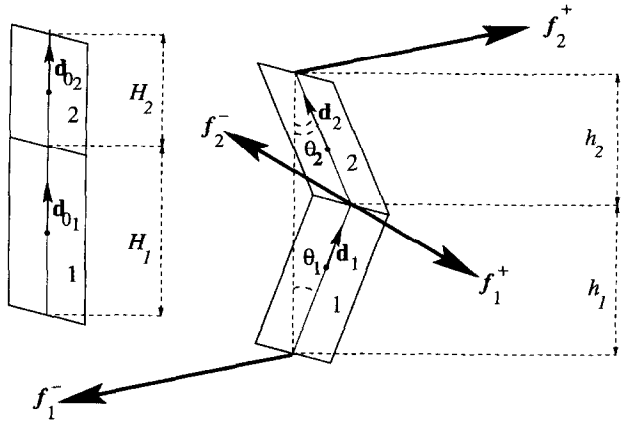

Fig. 4. Traction vectors $\mathbf{f}_\alpha^\pm$ ($\alpha = 1, 2$) (per unit initial length) acting on α-layers at the interface of the deformed material elements. Note that due to Y-periodicity, $\mathbf{f}_2^+ = -\mathbf{f}_1^-$ and due to continuity of the traction vector, $\mathbf{f}_2^- = -\mathbf{f}_1^+$.

$$\frac{h_1}{h_2} = \frac{H_1}{H_2} = \frac{v_1}{v_2}, \tag{2.12}$$

where v_1 and v_2 are the initial volume fractions of the layers such that $v_1 + v_2 = 1$. We can then rewrite (2.11) as†

$$v_1 \tan\theta_1 + v_2 \tan\theta_2 = 0. \tag{2.13}$$

2.3. *Distributed load factors hypothesis*

The governing rod equilibrium equations are

$$\mathbf{Q}' + \mathbf{q} = \mathbf{0}, \quad \mathbf{M}' + \mathbf{r}' \times \mathbf{Q} + \mathbf{m} = \mathbf{0}, \tag{2.14}$$

where $\mathbf{Q}$ and $\mathbf{M}$ are the vector force and vector moment acting on a cross-section and $\mathbf{q}$ and $\mathbf{m}$ are distributed load factors, respectively. For the two-dimensional problem under consideration, $\mathbf{M} = M\mathbf{k}$ and $\mathbf{m} = m\mathbf{k}$, where $\mathbf{k}$ is a unit vector orthogonal to the X–Y plane. Then, using (2.10), for each α-layer in the packet, we have

$$\mathbf{Q}_\alpha' + \mathbf{q}_\alpha = \mathbf{0}, \quad M_\alpha' + \mathbf{k} \cdot \mathbf{r}' \times \mathbf{Q}_\alpha + m_\alpha = 0, \quad \alpha = 1, 2, \tag{2.15}$$

where $\mathbf{q}_\alpha$ and m_α now represent the distributed forces and moments acting on each layer at the interfaces. Since the layer shapes are known in the initial configuration, we write our relations in terms of Lagrangian coordinates; the distributed loads $\mathbf{q}_\alpha$ and m_α, appearing in (2.15), are therefore expressed per unit initial length.

† Note that if the initial layer shape is only slightly curvilinear, then the angles of rotation are small, except for one case, namely where the stiffnesses of the layers differ greatly and the volume concentration of the weaker layer is very small. For example, let layer number 1 be the weaker layer with small volume concentration, $v_1 \ll 1$. (The limit case of this situation is a curvilinear crack.) Then from (2.13), we have $|\theta_1| \gg |\theta_2|$; however, since for this case the interaction between layers is clearly very weak, the angle θ_2 of the stiff layer approaches the angle of rotation of a *free* layer and, for an initial shape having only slight curviness, θ_2 is necessarily small. Thus, the relation (2.13) remains valid for moderate or large values of θ_1 where θ_1 can be considered as a function of θ_2. Furthermore, since for this case, θ_2 is small it can be approximately determined by linearization of the rod differential equation with respect to the angle.

Similarly we denote the actual traction vectors (per unit of the initial length) which act upon the upper and lower interface of each α-layer, respectively (Fig. 4), i.e. along the initial curves Γ_0, Γ_1, and Γ_2, by $\mathbf{f}_\alpha^+(S)$ and $\mathbf{f}_\alpha^-(S)$ ($\alpha = 1, 2$).

Due to the Y-periodicity, in the vertical direction, the tractions at the upper and the lower side of the packet must satisfy the relation

$$\mathbf{f}_2^+(S) = -\mathbf{f}_1^-(S). \tag{2.16}$$

Moreover, within the packet, the required *traction continuity* condition is clearly

$$\mathbf{f}_2^-(S) = -\mathbf{f}_1^+(S). \tag{2.17}$$

The distributed loads, therefore, are given by

$$\begin{aligned} \mathbf{q}_2(S) &= \mathbf{f}_2^+(S) + \mathbf{f}_2^-(S), \\ \mathbf{q}_1(S) &= \mathbf{f}_1^+(S) + \mathbf{f}_1^-(S) = -(\mathbf{f}_2^+(S) + \mathbf{f}_2^-(S)), \end{aligned} \tag{2.18}$$

and we arrive at the result

$$\mathbf{q}_1(S) + \mathbf{q}_2(S) = 0. \tag{2.19}$$

Adding the two force equilibrium equations together,

$$\sum_{\alpha=1}^{2} \mathbf{Q}_\alpha' + \sum_{\alpha=1}^{2} \mathbf{q}_\alpha = 0,$$

and using (2.19), we have

$$\sum_{\alpha=1}^{2} \mathbf{Q}_\alpha' = 0. \tag{2.20}$$

Using boundary condition ii, namely the absence of a shear force at the cell boundary, it follows that $\mathbf{Q}_1(S_L) = F_1\mathbf{i}$ and $\mathbf{Q}_2(S_L) = F_2\mathbf{i}$. Although F_1 and F_2 are unknown, their sum, $F = F_1 + F_2$, is precisely the force acting on a typical packet which can be related to the elongation. From (2.20), we therefore arrive at

$$\sum_{\alpha=1}^{2} \mathbf{Q}_\alpha(S) = F\mathbf{i}. \tag{2.21}$$

Note that this equation is a consequence of the periodicity and of the traction continuity condition. The validity of the relation is *not* restricted to the case of small deformations; it is equally valid for finite deformations.

We now seek a relation between the distributed moments m_1 and m_2 which is independent of the *unknown* traction forces at the interfaces. We first observe that the total distributed moment m_α produced by the traction forces at the interfaces is (Fig. 4)

$$\mathbf{m}_\alpha = \frac{h_\alpha \mathbf{d}_\alpha}{2\cos\theta_\alpha} \times (\mathbf{f}_\alpha^+ - \mathbf{f}_\alpha^-), \quad \text{no sum } (\alpha = 1, 2). \tag{2.22}$$

Due to the periodicity condition and the traction continuity at the interface, we have

$$\mathbf{f}_1^+ - \mathbf{f}_1^- = \mathbf{f}_2^+ - \mathbf{f}_2^- \equiv \mathbf{g}, \tag{2.23}$$

so that

$$\mathbf{m}_\alpha = \frac{h_\alpha \mathbf{d}_\alpha}{2\cos\theta_\alpha} \times \mathbf{g}, \text{ no sum.} \tag{2.24}$$

Representing $\mathbf{g}$ as

$$\mathbf{g} = g_x\mathbf{i} + g_y\mathbf{j}, \tag{2.25}$$

and taking into account (2.9) we arrive at

$$m_\alpha = -\frac{h_\alpha}{2}(g_x + g_y \tan\theta_\alpha), \text{ no sum.} \tag{2.26}$$

Here $\mathbf{m}_\alpha = m_\alpha \mathbf{k}$. We now adopt the following as **(force) hypothesis 4**:

$$|g_y \tan\theta_\alpha| \ll |g_x| \tag{2.27}$$

for all small and moderate θ_α, from which

$$\frac{m_\alpha}{h_\alpha} = -\frac{g_x}{2}, \text{ no sum.} \tag{2.28}$$

We then arrive at the critical approximate relation

$$\frac{m_1(S)}{h_1} = \frac{m_2(S)}{h_2}, \tag{2.29}$$

which, by (2.12) becomes

$$v_2 m_1 = v_1 m_2. \tag{2.30}$$

Using (2.30), we now multiply the moment equilibrium equation (2.15) for the first layer by v_2 and the equation for the second layer by v_1; upon subtracting the resulting expressions, we obtain

$$v_1 M_2' - v_2 M_1' + \mathbf{k} \cdot \mathbf{r}' \times (v_1 \mathbf{Q}_2 - v_2 \mathbf{Q}_1) = 0. \tag{2.31}$$

The force equilibrium equation (2.21) (two scalar equations), the moment equation (2.31) and the angle compatibility relation (2.13) are thus four equations for the four unknowns: the deformed shape $\mathbf{r}'$ and the two angles θ_1 and θ_2.

Alternatively, we note that since there exists a relation between the angles, the displacement of the double layer packet has one rotational and two translational degrees of freedom; equations (2.21) and (2.31) can then be considered as three scalar equations describing these degrees of freedom.

2.4. *The constitutive equations*

We represent the layers by means of an elastic geometrical nonlinear rod model under flexure, axial extension, and shear [see Eliseev (1988)]. The constitutive equations, applied to each α-rod, are

$$M_\alpha = c_\alpha \theta'_\alpha, \quad \mathbf{Q}_\alpha = \mathbf{b}_\alpha \boldsymbol{\Gamma}_\alpha, \quad \text{no sum} \quad (\alpha = 1, 2), \tag{2.32a, b}$$

where c_α denote the flexural rigidities, θ_α are the angles of the director rotations, defined by (2.5), and where the *strain* vectors

$$\boldsymbol{\Gamma}_\alpha = \mathbf{r}' - \mathbf{P}(\theta_\alpha)\mathbf{t}_0, \tag{2.33}$$

represent axial extension and shear deformation. Note that, here, we have used (2.7) and have invoked hypothesis ii, (2.10), i.e. $\mathbf{r}'$ is the common derivative of the radius vector to the deformed reference curves of the two α-rods. The symmetrical tensors $\mathbf{b}_\alpha$ are determined by the initial rigidity tensors $\mathbf{B}_\alpha$ as

$$\mathbf{b}_\alpha = \mathbf{P}(\theta_\alpha)\mathbf{B}_\alpha \mathbf{P}(\theta_\alpha)^{\mathrm{T}}, \quad \text{no sum} \quad (\alpha = 1, 2), \tag{2.34}$$

where $\mathbf{B}_\alpha = \mathbf{B}_\alpha(S)$ are symmetrical and positive definite tensors:

$$\mathbf{B}_\alpha = \mathbf{B}_\alpha^{\mathrm{T}}, \quad \mathbf{e} \cdot \mathbf{B}_\alpha \mathbf{e} > 0, \quad \text{for all } \mathbf{e}: \ |\mathbf{e}| = 1. \tag{2.35}$$

In accordance with our formulation, we choose to represent the rigidity tensor by

$$\mathbf{B}_\alpha = H_\alpha(E_\alpha \mathbf{i} \otimes \mathbf{i} + G_\alpha \mathbf{j} \otimes \mathbf{j}), \quad \text{no sum}, \tag{2.36}$$

where E_α and G_α ($\alpha = 1, 2$) are the effective Young's modulus and shear modulus of the α-layer. Note that this representation differs from the usual one [see Eliseev (1988)],

$$\mathbf{B}_\alpha = A_\alpha(E_\alpha \mathbf{t}_0 \otimes \mathbf{t}_0 + G_\alpha \mathbf{n}_0 \otimes \mathbf{n}_0), \ \text{no sum},$$

where A_α is the area of the cross-section perpendicular to $\mathbf{t}_0$. The differences with (2.36) lie in the difference of the principal directions of the tensors. This difference can be schematically illustrated as the difference in the orientations of the body-points at the reference line: the body-points are initially oriented normally to the reference line [Fig. 5(a)]; in our model the body-points in each layer have the same initial

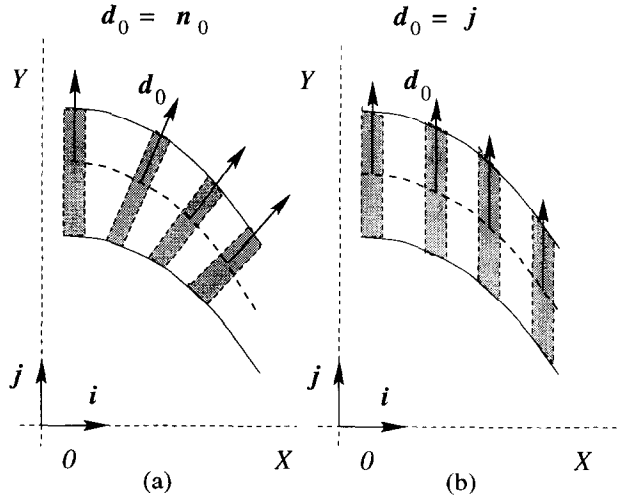

Fig. 5. Variant representations of the initial orientation of material elements.

orientation in the y-direction [Fig. 5(b)]. Further, we adopt the standard rod theory representation for the flexural rigidity†

$$c_\alpha = \frac{H_\alpha^3 E_\alpha}{12}, \text{ no sum } (\alpha = 1,2). \tag{2.37}$$

The force equilibrium equations for the packet, (2.21), are then written as

$$\mathbf{b}_1\boldsymbol{\Gamma}_1 + \mathbf{b}_2\boldsymbol{\Gamma}_2 = F\mathbf{i}. \tag{2.38}$$

3. SOLUTION TO THE SYSTEM OF EQUATIONS

3.1. *The general solution*

Substituting (2.33) in (2.38), we have

$$(\mathbf{b}_1 + \mathbf{b}_2)\mathbf{r}' - \mathbf{b}_1\mathbf{P}(\theta_1)\mathbf{t}_0 - \mathbf{b}_2\mathbf{P}(\theta_2)\mathbf{t}_0 = F\mathbf{i}, \tag{3.1}$$

from which

$$\mathbf{r}' = (\mathbf{b}_1 + \mathbf{b}_2)^{-1}(F\mathbf{i} + \mathbf{b}_1\mathbf{P}(\theta_1)\mathbf{t}_0 + \mathbf{b}_2\mathbf{P}(\theta_2)\mathbf{t}_0). \tag{3.2}$$

Using (2.34) and the identity $\mathbf{P}\mathbf{P}^{\mathrm{T}} = \mathbf{1}$ (where $\mathbf{1}$ is the unit tensor) we can finally write this relation as

$$\mathbf{r}' = (\mathbf{P}(\theta_1)\mathbf{B}_1\mathbf{P}^{\mathrm{T}}(\theta_1) + \mathbf{P}(\theta_2)\mathbf{B}_2\mathbf{P}^{\mathrm{T}}(\theta_2))^{-1}(F\mathbf{i} + \mathbf{P}(\theta_1)\mathbf{B}_1\mathbf{t}_0 + \mathbf{P}(\theta_2)\mathbf{B}_2\mathbf{t}_0). \tag{3.3}$$

We observe that the last expression yields an *explicit* form for $\mathbf{r}'$ as a function of the angles θ_α $(\alpha = 1,2)$.

Let us introduce the angle $\Omega = \Omega(S)$ which determines the initial tangent vector $\mathbf{t}_0$ to the template curve (2.2)

$$\mathbf{t}_0 = \mathbf{P}(\Omega)\mathbf{i}. \tag{3.4}$$

Using (2.3),

$$\Omega(0) = 0, \ \Omega(S_L) = 0. \tag{3.5}$$

Substituting (3.3) back into (2.33), we obtain the strain vectors $\boldsymbol{\Gamma}_\alpha$ $(\alpha = 1,2)$ as functions of the angles θ_α. Making use of (2.32a), equation (2.31) assumes a form

$$v_1 c_2 \theta_2'' - v_2 c_1 \theta_1'' + \Lambda_{12} = 0, \tag{3.6}$$

where

$$\Lambda_{12} = \mathbf{k} \cdot \mathbf{r}' \times (v_1\mathbf{Q}_2 - v_2\mathbf{Q}_1). \tag{3.7}$$

Here Λ_{12} depends on the unknowns θ_α $(\alpha = 1,2)$. Note that due to (2.21) and since $v_1 + v_2 = 1$, we have

† For rods of constant transverse thickness $\mathscr{H}$, the flexural rigidity is usually defined as $c = \mathscr{H}^3 E_\alpha/12$. In the present problem, the Y-thickness is constant, and we note the approximate relation $\mathscr{H} = \cos(\Omega)H_\alpha$, where Ω is the angle of inclination of the initial rod curve with respect to the X-axis. For small Ω there is no significant difference between this relation and $\mathscr{H} = H_\alpha$.

$$v_1\mathbf{Q}_2 - v_2\mathbf{Q}_1 = v_1(\mathbf{Q}_2+\mathbf{Q}_1) - (v_1+v_2)\mathbf{Q}_1 = v_1 F\mathbf{i} - \mathbf{Q}_1$$

and therefore

$$\Lambda_{12}(\theta_1, \theta_2; \Omega, F, \dots) = \mathbf{k}\cdot\mathbf{r}' \times (v_1 F\mathbf{i} - \mathbf{P}(\theta_1)\mathbf{B}_1\mathbf{P}^{\mathrm{T}}(\theta_1)\mathbf{r}' + \mathbf{P}(\theta_1)\mathbf{B}_1\mathbf{t}_0), \tag{3.8}$$

where $\mathbf{r}'$ is determined by (3.3). Here ellipses denote symbolically the material constants of the layers as well as the volume concentrations v_1 and v_2.

The relation (2.13) can be satisfied identically by letting

$$\begin{aligned} \theta_1 &= -\arctan(v_2\omega), \\ \theta_2 &= \arctan(v_1\omega), \end{aligned} \tag{3.9}$$

where the angle ω here represents a rotational degree of freedom of the double layer packet.

Due to the boundary conditions (2.4) along the material lines $X = 0$ and $X = L$, these material lines remain vertical in the process of deformation and consequently rotations necessarily vanish. We therefore arrive at the boundary conditions

$$\theta_\alpha(0) = 0, \ \theta_\alpha(S_L) = 0, \ \alpha = 1, 2, \tag{3.10}$$

and hence, from (3.9), we obtain

$$\omega(0) = 0, \ \omega(S_L) = 0. \tag{3.11}$$

Using (3.6) and (3.9), we finally write the governing equation as

$$D_2(\omega) + \tilde{\Lambda}_{12}(\omega; \Omega, F, \dots) = 0, \tag{3.12}$$

where

$$D_2(\omega) = (c_2 v_1 \arctan(v_1\omega) + c_1 v_2 \arctan(v_2\omega))''. \tag{3.13}$$

Here

$$\tilde{\Lambda}_{12}(\omega; \Omega, F, \dots) = \Lambda_{12}(\theta_1(\omega), \theta_2(\omega); \Omega, F, \dots). \tag{3.14}$$

Thus, (3.12) which represents the final governing equation of the problem, is a nonlinear ODE of second order subjected to the boundary conditions (3.11).

Note that for the case of equal volume concentrations, $v_1 = v_2 = 1/2$, the relation between the angles θ_1 and θ_2 is simplified:

$$\theta_1 = -\theta_2, \quad \text{if } v_1 = v_2 = \frac{1}{2}, \tag{3.15}$$

and equation (3.6), together with the boundary conditions (3.10), takes the simpler form

$$\frac{1}{2}(c_2 + c_1)\theta_2'' + \hat{\Lambda}_{12}(\theta_2; \Omega, F, \dots) = 0, \ \theta_2(0) = 0, \ \theta_2(S_L) = 0. \tag{3.16}$$

Here

$$\hat{\Lambda}_{12}(\theta_2; \Omega, F, \dots) \equiv \Lambda_{12}(-\theta_2, \theta_2; \Omega, F, \dots). \tag{3.17}$$

Upon determining the angles, we can then calculate $\mathbf{r}'$ by (3.3) and, by integration, find the new shape of the packet. In particular, the relation between the actual half-period l of the packet with respect to the x-coordinate and the applied average extensional load F is given by

$$l = \int_0^{S_L} \mathbf{i} \cdot \mathbf{r}'(\theta_1, \theta_2; \Omega, F, \ldots) \mathrm{d}S. \tag{3.18}$$

3.2. *The limit case of the homogeneous material*

It is of interest to discuss the limit case, namely where the layers consist of the same material, in which case the composite behaves as a homogeneous material. In this case, under tension in the X-direction, the solution is represented by constant stress and strain fields and no rotation along *any* vertical lines can occur. We now demonstrate that our general analysis leads directly to this physical state.

We first note that the initial rigidity tensors $\mathbf{B}_\alpha$ are proportional to the volume concentrations v_α ($\alpha = 1, 2$). Let $\mathbf{B}_0$ be the rigidity tensor of a rod with Y-thickness, H, $H = H_1 + H_2$. Since the material in both layers is the same, we have

$$\mathbf{B}_1 = v_1 \mathbf{B}_0, \quad \mathbf{B}_2 = v_2 \mathbf{B}_0. \tag{3.19}$$

Thus, owing to the constitutive relation (2.32), (2.33) and (2.34),

$$\mathbf{Q}_\alpha = \mathbf{b}_\alpha \mathbf{\Gamma}_\alpha, \quad \mathbf{b}_\alpha = v_\alpha \mathbf{P}(\theta_\alpha) \mathbf{B}_0 \mathbf{P}^{\mathrm{T}}(\theta_\alpha), \quad \mathbf{\Gamma}_\alpha = \mathbf{r}' - \mathbf{P}(\theta_\alpha)\mathbf{t}_0, \quad \text{no sum.} \tag{3.20}$$

Now, in principle, one can construct $\mathbf{r}'$ by (3.3) and, using (3.8) and (3.9), obtain $\tilde{\Lambda}_{12}$ given by (3.14).

This process leads to rather complex algebraic manipulations and a detailed investigation of the resulting nonlinear ODE. Instead, let us assume that the problem for the homogeneous material has a *unique* solution, namely as mentioned above, that no rotations occur at any points and that the resulting stress and strain fields are constant. We then need only show that

$$\theta_1(S) = 0, \ \theta_2(S) = 0, \ \text{for any } S \tag{3.21}$$

are a solution to the homogeneous problem. To satisfy (3.6) we require, in this case, that

$$\mathbf{k} \cdot \mathbf{r}' \times (v_1 \mathbf{Q}_2 - v_2 \mathbf{Q}_1) = 0. \tag{3.22}$$

Noting that $\mathbf{P}(0) = \mathbf{1}$, the unit tensor, and using (3.19)–(3.21), we have

$$\begin{aligned} &\mathbf{\Gamma}_1 = \mathbf{\Gamma}_2 = \mathbf{r}' - \mathbf{t}_0, \\ &\mathbf{Q}_1 = v_1 \mathbf{Q}_0, \ \mathbf{Q}_2 = v_2 \mathbf{Q}_0, \quad \text{where } \mathbf{Q}_0 = \mathbf{B}_0(\mathbf{r}' - \mathbf{t}_0). \end{aligned} \tag{3.23}$$

Thus we obtain

$$v_1 \mathbf{Q}_2 - v_2 \mathbf{Q}_1 = 0, \tag{3.24}$$

and hence (3.22) is satisfied.

Let us now consider the displacement field. Noting again that $v_1+v_2=1$, due to (2.21) and (3.23) we have

$$\mathbf{B}_0(\mathbf{r}'-\mathbf{t}_0)=F\mathbf{i}. \tag{3.25}$$

In passing, we observe that (3.3) leads to this same result. Since $\mathbf{t}_0=\mathbf{r}_0'$ and

$$\mathbf{u}=\mathbf{r}-\mathbf{r}_0 \tag{3.26}$$

defines the *displacement* vector of a reference line, from (3.25) we have

$$\mathbf{u}'=F\mathbf{B}_0^{-1}\mathbf{i}. \tag{3.27}$$

Since the materials of the layers are the same, $E_1=E_2\equiv E$, $G_1=G_2\equiv G$, and since $\mathbf{B}_0=\mathbf{B}_1+\mathbf{B}_2$, using (2.36), we obtain

$$\mathbf{B}_0=H(E\mathbf{i}\otimes\mathbf{i}+G\mathbf{j}\otimes\mathbf{j}),\quad H=H_1+H_2, \tag{3.28}$$

or

$$\mathbf{B}_0^{-1}=H^{-1}(E^{-1}\mathbf{i}\otimes\mathbf{i}+G^{-1}\mathbf{j}\otimes\mathbf{j}). \tag{3.29}$$

Since $F=H\sigma_0$ and $\sigma_0=E\varepsilon_0$, where σ_0 is the only component of the unidirectional *constant* stress field, $\boldsymbol{\sigma}=\sigma_0\mathbf{i}\otimes\mathbf{i}$, and ε_0 denotes the ε_{xx} component of the strain tensor produced by the stress field,

$$F=HE\varepsilon_0. \tag{3.30}$$

Substituting (3.29) and (3.30) into (3.27) we have

$$\mathbf{u}'=\varepsilon_0\mathbf{i}. \tag{3.31}$$

Note that $\mathbf{u}'\equiv \mathrm{d}\mathbf{u}/\mathrm{d}S$, and since $\mathrm{d}X=\cos\Omega\mathrm{d}S$, we can write (3.31) as

$$\frac{\mathrm{d}\mathbf{u}}{\mathrm{d}X}=\cos(\Omega)\varepsilon_0\mathbf{i}. \tag{3.32}$$

Comparing this solution with the displacement field under unidirectional tension in a homogeneous isotropic elastic body, we observe that it differs from the *exact* expression for u_x by terms of order $\varepsilon_0\Omega^2$, which for $|\Omega|\ll 1$, are of the *third* order. As we shall show in the analytical solution (of Section 4), the geometrical nonlinearity in behavior which appears if the layers have significantly different properties, is only of second order, i.e. Ω^2. Thus, we achieve sufficient accuracy in the homogeneous problem.

We note, however, the absence of shrinking of the material in the Y-direction due to the elongation in the X-direction, i.e. $u_y\equiv 0$ in solution (3.32). This *defect* of our theory is to be expected since in the rod theory as developed here, we have neglected the *degree of freedom* representing thickness changes.

3.3. *The limit case* $H/L\to 0$

It is known that the mathematical theory of homogenization of periodic structures can be formulated in terms of the asymptotical behavior of a solution if the size of

the structural element approaches zero [see Bensoussan *et al.* (1988)]. In our case this corresponds to the limit $H/L \to 0$.

Since the flexural rigidities (2.37) are to the *third* degree with respect to H and the stiffness matrices $\mathbf{B}_\alpha$ $(\alpha = 1, 2)$ (2.36) are to the *first* degree, upon introducing a nondimensional arc length, $\tilde{S} = S/S_L \in [0, 1]$, we can write (3.6) in the following nondimensional form:

$$\frac{1}{12}\left(\frac{H}{L}\right)^2 \frac{\mathrm{d}^2}{\mathrm{d}\tilde{S}^2}\left(v_1 v_2^3 \frac{E_2}{E_1+E_2}\theta_2 + v_2 v_1^3 \frac{E_1}{E_1+E_2}\theta_1\right) + \left(\frac{S_L}{L}\right)^2 \frac{\Pi_{12}(\theta_1, \theta_2; \Omega, \sigma, \dots)}{E_1+E_2} = 0, \tag{3.33}$$

where θ_1 and θ_2 are related by (2.13). Here we have used the obvious relation between stress σ and the force $F = H\sigma$, and

$$\Pi_{12}(\theta_1, \theta_2; \Omega, \sigma, \dots) = H^{-1}\Lambda_{12}(\theta_1, \theta_2; \Omega, H\sigma, \dots). \tag{3.34}$$

Since Λ_{12} is a homogeneous function in H of first degree, we observe that Π_{12} depends only on σ and not on H; note too that $S_L/L \sim 1$.

The ODE (3.33) is clearly *singular* since the small parameter H/L is attached to the highest derivative. Thus, except near the ends $S = 0$ and $S = S_L$, we can expect the solution to behave as a solution of the system defined by the *transcendental* equation

$$\Pi_{12}(\theta_1, \theta_2; \Omega, \sigma, \dots) = 0 \tag{3.35}$$

and (2.13)†.

It is also known from the general theory of singular equations that one can formally expect the existence of boundary layers if the solutions of (3.33) and (2.13) are incompatible with the boundary conditions of the equation. However, we now show that the boundary conditions (3.10) are compatible with the system (3.35) and (2.13) and hence the solution of (3.35) and (2.13) approximates the solution in the *entire* interval $S = [0, S_L]$. Specifically, we require that Λ_{12} vanish at $S = 0$ and $S = S_L$. To demonstrate this we need only show that

$$\mathbf{Q}_\alpha(0) = \sim \mathbf{i}, \quad \mathbf{Q}_\alpha(S_L) = \sim \mathbf{i}, \quad (\alpha = 1, 2), \tag{3.36}$$

and

$$\mathbf{r}'(0) = \sim \mathbf{i}, \quad \mathbf{r}'(S_L) = \sim \mathbf{i}, \tag{3.37}$$

since this then guarantees that the vector product (3.7) is zero. Here, the symbol "$= \sim$" means "parallel to".

We first substitute $\theta_1 = 0$ and $\theta_2 = 0$ into (3.3). Since at the boundaries $\mathbf{t}_0 = \mathbf{i}$, we arrive at (3.37). Using the same value for θ_1 and θ_2 together with the relation of (3.37) and making use of (2.33)–(2.36), we arrive at (3.36).

Therefore, *no* boundary layers exist in the solution and accordingly the solution of the system (3.35) and (2.13) is asymptotically valid in the *entire* interval $S = [0, S_L]$. Hence for the case $H/L \ll 1$, $\Pi_{12} = 0$ [together with (2.13)] yields solutions that are valid in the entire interval.

† On the other hand, introducing ω according to (3.9) somewhat simplifies the analysis of the system by reducing it to one transcendental equation.

4. ANALYTICAL SOLUTION FOR SMALL INITIAL WAVINESS

4.1. *Determination of angles of rotation*

We consider here the case of small initial waviness, i.e.,

$$|\Omega| \ll 1. \tag{4.1}$$

It is clear that the angles θ_1 and θ_2 are then also small. Performing linearization of Λ_{12}, (3.8), with respect to θ_α and Ω, [where $\mathbf{r}'$ is given by (3.3)], we obtain [see (A.19) of Appendix A]

$$\Lambda_{12} = -v_1 v_2 H((1+\varepsilon)G^{-1}G_1G_2(\theta_2-\theta_1)+(\Omega+\bar{\theta})(E_2-E_1)\varepsilon), \tag{4.2}$$

where, here and below, we use the following notation:

$$\begin{aligned} &G = v_1G_1+v_2G_2, \quad E = v_1E_1+v_2E_2,\\ &\bar{\theta} = G^{-1}(g_1\theta_1+g_2\theta_2),\\ &g_\alpha = v_\alpha G_\alpha, \quad f_\alpha = v_\alpha E_\alpha, \quad \text{no sum}(\alpha = 1,2), \end{aligned} \tag{4.3}$$

and

$$\varepsilon = \frac{F}{EH} \tag{4.4}$$

and where G and E are the "averages" of the shear modulus and the Young's modulus in the simple sense: i.e. $< \mathrm{A} > \equiv v_1A_1+v_2A_2$ for any constant A.

Linearization of the relation between θ_1 and θ_2, (2.13) leads to

$$v_1\theta_1+v_2\theta_2 = 0, \tag{4.5}$$

which can be satisfied by letting

$$\theta_1 = -v_2\omega, \quad \theta_2 = v_1\omega. \tag{4.6}$$

From (4.3) and (4.6),

$$\bar{\theta} = v_1v_2G^{-1}(G_2-G_1)\omega. \tag{4.7}$$

Finally, using (4.2), (4.6) and (4.7), we represent the linearized $\tilde{\Lambda}_{12}(\omega;\ \Omega,\varepsilon,\dots)$, (3.14), as

$$\tilde{\Lambda}_{12}(\omega;\Omega,\varepsilon,\dots) = -\Lambda\omega-K_0\Omega, \tag{4.8}$$

where

$$\Lambda = v_1v_2H((1+\varepsilon)G^{-1}G_1G_2+v_1v_2G^{-1}(G_2-G_1)(E_2-E_2)\varepsilon) \tag{4.9}$$

and

$$K_0 = v_1v_2H(E_2-E_1)\varepsilon \tag{4.10}$$

are constants. It is important to note that Λ is always positive under extension, $\varepsilon > 0$ [see proof in Appendix (A.6)].

Linearizing (3.13) with respect to ω, we write (3.12) as

$$(v_1^2 c_2 + v_2^2 c_1)\omega'' - \Lambda\omega - K_0\Omega = 0, \tag{4.11}$$

i.e.,†

$$C\omega'' - \Lambda\omega = K_0\Omega, \tag{4.12}$$

where, from (2.37),

$$C = v_1^2 \frac{H_2^3 E_2}{12} + v_2^2 \frac{H_1^3 E_1}{12}.$$

Finally, using $H_\alpha = v_\alpha H$ ($\alpha = 1, 2$) and (4.3) we obtain

$$C = v_1^2 v_2^2 \frac{(v_2 E_2 + v_1 E_1)H^3}{12} = v_1^2 v_2^2 \frac{EH^3}{12}. \tag{4.13}$$

Now, Ω is usually given as a function of X and not of S. The exact relation, via the template curve (2.2) is

$$\tan(\Omega) = \frac{\mathrm{d}Y_0(X)}{\mathrm{d}X}, \tag{4.14}$$

which, in linearized form, is

$$\Omega = \frac{\mathrm{d}Y_0(X)}{\mathrm{d}X}. \tag{4.15}$$

Since

$$\frac{\mathrm{d}S}{\mathrm{d}X} = \cos\Omega \sim 1 - \frac{\Omega^2}{2},$$

and neglecting the cubic-order terms, we replace ω'' in (4.12) by $(\mathrm{d}^2\omega)/(\mathrm{d}X^2)$. Assuming now $\omega = \omega(X)$ and noting that $X = L$ corresponds to $S = S_L$, we write the boundary conditions (3.11) as

$$\omega(0) = 0, \quad \omega(L) = 0. \tag{4.16}$$

The solution of the ODE (4.12) with the boundary conditions (4.16) for *arbitrary* Ω is

$$\omega(X) = \frac{K_0}{C}\int_0^L G(X, T)\Omega(T)\mathrm{d}T, \tag{4.17}$$

where the Green function $G(X, T)$ is given by‡

† In the limit case $G_1/G_2 \to 0$ and $E_1/E_2 \to 0$, this equation approaches the free rod equation $c_2\theta_2'' - H_2E_2\varepsilon(\theta_2 + \Omega) = 0$ for the second layer.

‡ It is clear that $G(X, T)$ satisfies the equation $(\mathrm{d}^2G)/(\mathrm{d}X^2) - \lambda^2 G = 0$ for $X \neq T$ for zero boundary conditions and that $G(X, T)$ is continuous at the point $X = T$ with a jump of the first derivative, $[(\mathrm{d}G)/(\mathrm{d}X)] = 1$. Thus, G is the Green function for $(\mathrm{d}^2G)/(\mathrm{d}X^2) - \lambda^2 G = \delta(X - T)$.

$$G(X,T)=\begin{cases}\dfrac{\sinh(\lambda X)\sinh[\lambda(L-T)]}{\lambda\sinh(\lambda L)}, & \text{if } X<T,\\[2ex] \dfrac{\sinh[\lambda(L-X)]\sinh(\lambda T)}{\lambda\sinh(\lambda L)}, & \text{if } X>T,\end{cases} \tag{4.18}$$

with

$$\lambda=(C^{-1}\Lambda)^{1/2}. \tag{4.19}$$

Consider the simplest case, where Ω is sinusoidal:

$$\Omega=-\Omega_0\sin\left(\pi\frac{X}{L}\right); \tag{4.20}$$

this case corresponds to a cosinusoidal template curve (with small waviness),

$$Y_0=A\cos\left(\pi\frac{X}{L}\right), \tag{4.21}$$

where the relation between Ω_0 and the initial cosine amplitude A is

$$\Omega_0=\pi A. \tag{4.22}$$

The solution of (4.12) with boundary conditions (4.16) is

$$\omega(X)=-\frac{K_0}{\dfrac{\pi^2}{L^2}C+\Lambda}\Omega_0\sin\left(\pi\frac{X}{L}\right), \tag{4.23}$$

or in an abbreviated form

$$\omega(X)=-K\Omega(X), \tag{4.24}$$

where, using (4.9), (4.10), and (4.13),

$$K=\frac{(E_2-E_1)\varepsilon}{\pi^2 12^{-1}v_1v_2E\dfrac{H^2}{L^2}+(1+\varepsilon)G^{-1}G_1G_2+v_1v_2G^{-1}(G_2-G_1)(E_2-E_1)\varepsilon}. \tag{4.25}$$

4.2. *Determination of the deformed layers shape*

Expanding (3.3) in a Taylor series with respect to θ_1 and θ_2 and using the notation of (4.3), we obtain† (see Appendix A.3)

† Noting that G and E can also be written as $G=g_1+g_2$ and $E=f_1+f_2$, for the case $f_1\ll f_2$ and $g_1\ll g_2$, (4.26) approaches

$$x'=1+\varepsilon-\frac{(\Omega+\theta_2)^2}{2},$$

$$y'=\Omega+\theta_2.$$

$$x' = 1+\varepsilon-\frac{\Omega^2}{2}-E^{-1}(f_1\theta_1+f_2\theta_2)\Omega+\beta(\theta_1,\theta_2),$$

$$y' = \Omega+\bar{\theta}. \tag{4.26a}$$

where β, representing second order terms, is given by

$$\beta(\theta_1,\theta_2) = E^{-1}G^{-1}\left(-\frac{1}{2}f_1g_1+\frac{1}{2}f_1g_2-g_1g_2\right)\theta_1^2$$

$$+E^{-1}G^{-1}\left(-\frac{1}{2}f_2g_2+\frac{1}{2}f_2g_1-g_1g_2\right)\theta_2^2$$

$$+E^{-1}G^{-1}(-f_1g_2-f_2g_1+2g_1g_2)\theta_1\theta_2. \tag{4.26b}$$

Here x' is written to *second* degree accuracy†, i.e. the remainder is $O([\theta_1,\theta_2,\Omega,\varepsilon],3)$, and y' is written with *linear* accuracy, i.e. the remainder is $O([\theta_1,\theta_2,\Omega,\varepsilon]2)$.

Substituting the relations (4.6) into (4.26), the resulting expressions have the structure

$$x' = 1+\varepsilon-\frac{\Omega^2}{2}-A_x\omega\Omega+B_x\omega^2,$$

$$y' = \Omega+A_y\omega, \tag{4.27}$$

where A_x, B_x, and A_y are constants which are determined below. Here x' and y' are the derivatives with respect to S. Since $\mathrm{d}X = \cos(\Omega)\mathrm{d}S$, we then have with corresponding accuracy (quadratic for x' and linear for y')

$$\frac{\mathrm{d}x}{\mathrm{d}X} = 1+\varepsilon-A_x\omega\Omega+B_x\omega^2,$$

$$\frac{\mathrm{d}y}{\mathrm{d}X} = \Omega+A_y\omega. \tag{4.28}$$

Comparing (4.26a) and (4.27) and using (4.7), we have

$$A_y = v_1v_2G^{-1}(G_2-G_1). \tag{4.29}$$

Similarly, using (4.6),

$$A_x = v_1v_2E^{-1}(E_2-E_1). \tag{4.30}$$

To calculate B_x, we first note that $B_x\omega^2 = \beta(-v_2\omega, v_1\omega)$, where β is given by (4.26b). Then, after some manipulation, collecting coefficients of ω^2, we finally obtain

$$B_x = v_1v_2E^{-1}G^{-1}\left[\frac{v_2G_2-v_1G_1}{2}(v_2E_1-v_1E_2)+v_1v_2(E_1G_2+E_2G_1)-G_1G_2\right]. \tag{4.31}$$

† We employ the notation $O([a_1^{\alpha_1}a_2^{\alpha_2}\ldots a_M^{\alpha_M}y],N)$ to designate all terms $O(a_1^{\alpha_1}a_2^{\alpha_2}\ldots a_M^{\alpha_M}y)$ such that $\Sigma_{i=1}^{M}\alpha_i = N$.

Once $\omega(X)$ has been determined by (4.17), we obtain $x = x(X)$ and $y = y(X)$ by integration of (4.28):

$$x(X) = \int_0^X \frac{\mathrm{d}x}{\mathrm{d}X}\mathrm{d}X, \quad y(X) = const + \int_0^X \frac{\mathrm{d}y}{\mathrm{d}X}\mathrm{d}X,$$

where we have used the boundary condition $x(0) = 0$. Note that no boundary condition exists for $y(0)$; the translation in the Y-direction is *arbitrary* and is not constrained by the force boundary condition. Therefore, generally speaking, the constant is arbitrary. Since x and y are coordinates of the deformed template curve, we can always assume that the initial template curve (2.2) satisfies

$$\int_0^L Y_0(X)\mathrm{d}X = 0,$$

and thus determine the constant by demanding that

$$\int_0^L y(X)\,\mathrm{d}X = 0.$$

If, in particular, $\Omega(X)$ is sinusoidal, using relation (4.24) we have

$$\frac{\mathrm{d}x}{\mathrm{d}X} = 1 + \varepsilon + (A_x K + B_x K^2)\Omega^2,$$

$$\frac{\mathrm{d}y}{\mathrm{d}X} = (1 - A_y K)\Omega. \tag{4.32}$$

Performing the integration we obtain

$$x(X) = \left(1 + \varepsilon + \frac{\Omega_0^2}{2}(A_x K + B_x K^2)\right)X - \frac{\Omega_0^2 L}{4\pi}(A_x K + B_x K^2)\sin\left(2\pi\frac{X}{L}\right)$$

$$y(X) = (1 - A_y K)\pi^{-1}\Omega_0 L\cos\left(\pi\frac{X}{L}\right). \tag{4.33}$$

We observe that the function $y(X)$,

$$y = a\cos\left(\pi\frac{X}{L}\right), \tag{4.34}$$

has the same shape as $Y_0(X)$, (4.21), but with different amplitude. From (4.22) and (4.33), we then obtain

$$\frac{a}{A} = 1 - A_y K, \tag{4.35}$$

which, using (4.25), we can write explicitly as

$$\frac{a}{A}=\frac{\pi^2 12^{-1}v_1v_2\dfrac{H^2}{L^2}+(1+\varepsilon)E^{-1}G^{-1}G_1G_2}{\pi^2 12^{-1}v_1v_2\dfrac{H^2}{L^2}+(1+\varepsilon)E^{-1}G^{-1}G_1G_2+v_1v_2E^{-1}G^{-1}(G_2-G_1)(E_2-E_1)\varepsilon}. \tag{4.36}$$

We remark that this relation for the relative amplitude does not depend on Ω_0. We note, however, that in the above analysis, Ω_0 has been considered to be small; for moderate Ω_0, as will be shown by numerical calculations (in Section 5), there exists a weak dependence on Ω_0.

4.3. *Force–elongation relation*

The relative elongation of the packet in the X-direction,

$$\bar{\varepsilon}=\frac{l-L}{L} \tag{4.37}$$

can be also represented as

$$\bar{\varepsilon}=\left\langle\frac{\mathrm{d}x}{\mathrm{d}X}\right\rangle-1; \tag{4.38}$$

here $\langle\ldots\rangle$ denotes the averaging $\langle f\rangle=L^{-1}\int_0^L f\,\mathrm{d}X$.

The aim here is to obtain $\bar{\varepsilon}=\bar{\varepsilon}(F)$ or, using (4.4), $\bar{\varepsilon}=\bar{\varepsilon}(\varepsilon)$. We first observe that $\mathrm{d}x/\mathrm{d}X$ is a function of ε and ω. For any *arbitrary* initial shape of the template curve, this problem can then be solved using Green functions given by (4.18). Owing to (4.28) and (4.17) we then have

$$\bar{\varepsilon}=\varepsilon-A_xI_1(\varepsilon)+B_xI_2(\varepsilon), \tag{4.39}$$

where, noting that the Green function (4.18) depends on ε via λ [see (4.19) and (4.9)],

$$I_1(\varepsilon)=\frac{K_0}{C}\frac{1}{L}\int_0^L\int_0^L G(T',T)\Omega(T)\Omega(T')\mathrm{d}T\,\mathrm{d}T',$$

$$I_2(\varepsilon)=\frac{K_0^2}{C^2}\frac{1}{L}\int_0^L\int_0^L P(T',T)\Omega(T)\Omega(T')\mathrm{d}T\,\mathrm{d}T', \tag{4.40}$$

where the symmetrical kernel $P(T,T')$ is defined as

$$P(T,T')=\int_0^L G(X,T)G(X,T')\,\mathrm{d}X. \tag{4.41}$$

We observe that the integrals of (4.40) are of second degree in Ω.

In the particular case of a cosinusoidal initial shape, due to (4.33) and (4.37), we have

$$\bar{\varepsilon}(\varepsilon) = \varepsilon + \frac{\Omega_0^2}{2}(A_x K + B_x K^2) \tag{4.42}$$

where $K = K(\varepsilon)$ is represented by (4.25) and A_x and B_x are given by (4.30) and (4.31), respectively. Here we note that $\bar{\varepsilon}$ depends explicitly on the second order of Ω_0.

Some simplifications of the relations for A_x, A_y, B_x and K can be achieved in the case of equal Poisson's ratios (see Appendix B).

5. NUMERICAL RESULTS AND DISCUSSION

In this section, we first present numerical results for the nonlinear problem formulated in Section 3 and compare with the approximate analytical solution derived in Section 4.

As a typical case of a wavy composite, we shall assume that the initial shape of the template curve is cosinusoidal:

$$Y_0(X) = A\cos\left(\pi\frac{X}{L}\right). \tag{5.1}$$

The initial inclination, $\Omega(X)$ with respect to the axis X is then

$$\Omega(X) = -\arctan\left(\frac{\pi A}{L}\sin\left(\pi\frac{X}{L}\right)\right), \tag{5.2}$$

and hence its maximal value is

$$\Omega_0 = \arctan\left(\frac{\pi A}{L}\right). \tag{5.3}$$

Let

$$l_* = \int_0^L (1 + (\mathrm{d}Y/\mathrm{d}X)^2)^{1/2}\mathrm{d}X \tag{5.4}$$

denote the original arc length of the layer contained within a typical half-cell ($0 \leqslant X \leqslant L$). Observing that l_* corresponds to pure geometrical straightening of the template curve along the X-axis with no axial strain, the corresponding relative elongation [see (4.37)] is then

$$\bar{\varepsilon}_* = \frac{l_* - L}{L}.$$

By integrating (3.16) numerically and using (3.15) (the volume concentrations are assumed to be equal, $v_1 = v_2 = 0.5$), the angles of rotation θ_1 and θ_2, are first obtained.

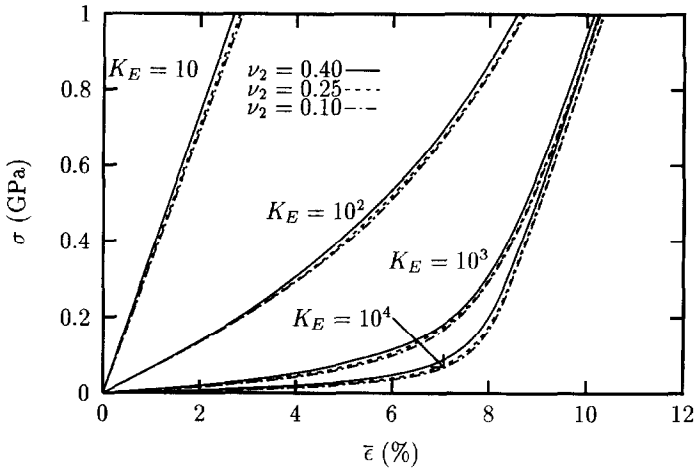

Fig. 6. Effect of Poisson's ratio on stress–(macro) strain curves for typical values of $K_E = E_2/E_1$; $v_1 = v_2 = 0.5$, $K_H = 0.05$, $\Omega_0 = 30°$, $v_1 = 0.40$.

The x' and y' components of $\mathbf{r}'$, determined by (3.3), are then substituted in

$$\bar{\varepsilon} = \frac{\int_0^{S_L} x' \mathrm{d}S}{L} - 1, \quad a = -\frac{\int_0^{S_L} y' \mathrm{d}S}{2}; \tag{5.5a, b}$$

which, integrated numerically, determines the "macro" strain $\bar{\varepsilon}$ and the amplitude a of the layers in the deformed state. Note that, in the above, $S_L = l_*$.

Clearly, the initially cosinusoidal template curve (5.1) after deformation is no longer purely cosinusoidal; therefore the term "amplitude" as defined in (5.5b) by the simple rule $[y(0) - y(S_L)]/2$, is used here in the loose sense. Nevertheless, this quantity can help to describe qualitatively the inner processes of the deformation of the template curve†. Note that in the initial state $a = A$ and for a straight template curve $a = 0$.

In presenting the results below, we shall consider layer 2 to be the stiffer layer. We first show the relation between the stress, σ, and macro strain, $\bar{\varepsilon}$, for several values of the Poisson's ratio of the stiffer layer, v_2, and for various ratios of the Young's moduli of the layers, K_E, with a given value of the relative thickness of the packet, K_H:

$$K_E = E_2/E_1, \quad K_H = H/L. \tag{5.6}$$

The corresponding σ–$\bar{\varepsilon}$ curves are shown in Fig. 6 for material constants‡ $E_2 = 100$

† It is intuitively clear that the deformed template curve (corresponding to the initially cosinusoidal shape) decreases monotonically from $y(0)$ to $y(S_L)$, and therefore $a = \|y\|$. Now, the template curve evidently preserves the central symmetry with respect to the material point $(X, Y) = [S_L/2, y(S_L/2)]$. Thus the amplitude which we have introduced is the maximum value of the function $f(S) = y(S) - y(S_L/2)$ and therefore it is, in fact, its L_∞ norm.

‡ Since the plane problem is under consideration, for any given material, E_α and v_α, the stiffness matrices $\mathbf{B}_\alpha$ ($\alpha = 1, 2$) are calculated according to the plane strain relations [see, e.g., Little (1973) or Fraeijs de Veubeke (1979)] using the effective Young's moduli and shear moduli

$$\frac{E_\alpha}{1 - v_\alpha^2} \quad \text{and} \quad \frac{E_\alpha}{2(1 - v_\alpha)} \ (\alpha = 1, 2) \ \text{(no sum)},$$

respectively.

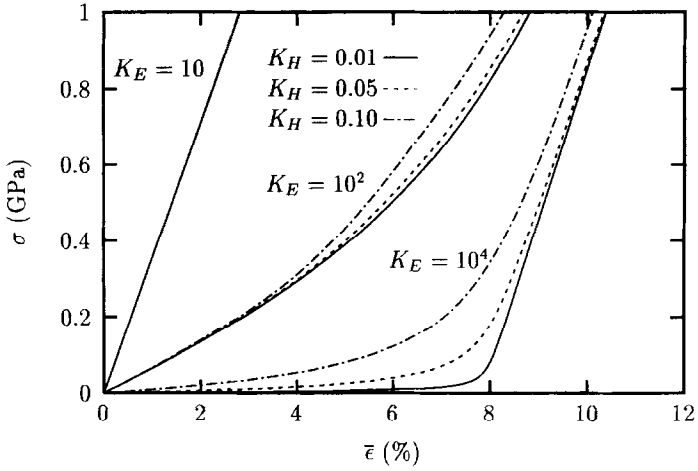

Fig. 7. Effect of $K_H = H/L$ on stress–(macro) strain curves for some typical values of $K_E = E_2/E_1$; $v_1 = v_2 = 0.5$, $\Omega_0 = 30°$.

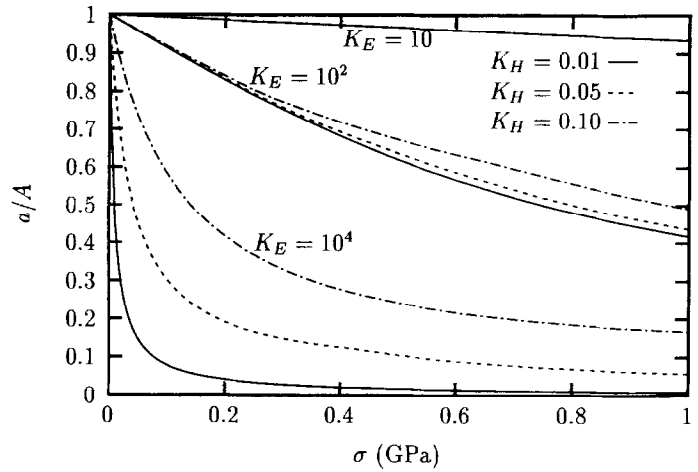

Fig. 8. Amplitude–stress curves for typical values of $K_E = E_2/E_1$, $K_H = H/L$; $v_1 = v_2 = 0.5$, $\Omega_0 = 30°$.

GPa, $v_2 = \{0.10, 0.25, 0.40\}$, $K_E = \{10, 10^2, 10^3, 10^4\}$ and $v_1 = 0.40$; the maximal initial angle is taken as $\Omega_0 = 30°$, $K_H = 0.05$, and the volume concentrations are assumed to be equal, $v_1 = v_2 = 0.5$. We observe that the behavior depends strongly on K_E but, for any given K_E, is almost *independent* of the Poisson's ratio. Thus, in the further investigation we choose the specific values $v_1 = 0.40$ and $v_2 = 0.25$ and will concentrate our attention on the influence of the parameters K_E and K_H. In choosing a value for v_1 we have been guided from experience that the weaker layer in a composite, i.e. the *matrix*, is usually made of a slightly compressible material such as a polymer.

Figures 7–10 describe the response of the wavy composite under tension using different variables. In each figure, the tension process is represented for typical parameters $K_E = \{10, 10^2, 10^4\}$ and $K_H = \{0.01, 0.05, 0.1\}$. Figure 7 shows the σ–$\bar{\varepsilon}$ curves

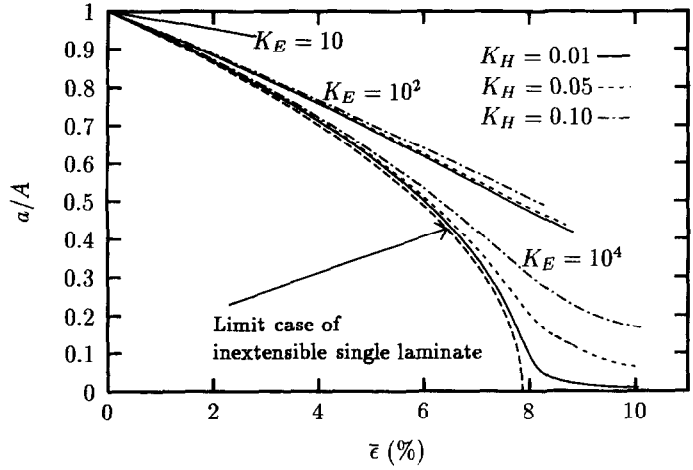

Fig. 9. Amplitude–(macro) strain curves for typical values of $K_E = E_2/E_1$, $K_H = H/L$; $v_1 = v_2 = 0.5$, $\Omega_0 = 30°$.

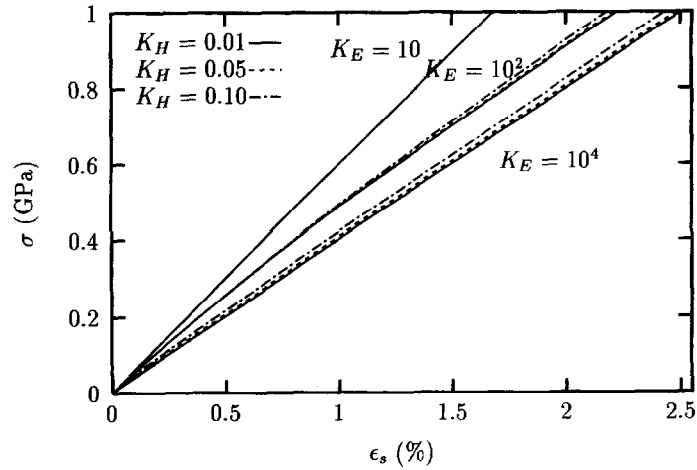

Fig. 10. The σ–ε_s curves for typical values of $K_E = E_2/E_1$, $K_H = H/L$; $v_1 = v_2 = 0.5$, $\Omega_0 = 30°$.

in the range $\sigma \in [0, 1]$ GPa. For values $K_E = 10^2$ and $K_E = 10^4$ the behavior is significantly nonlinear, while for $K_E = 10$ the relation approaches linear behavior. Moreover, we observe that for $K_E = 10$, the behavior is independent of the parameter K_H (the curves for several values of K_H effectively coincide in Figs 7–10). However, for larger values of K_E, $K_E = 10^2$ and $K_E = 10^4$, the parameter K_H has an increasingly greater influence. We observe that for $K_E = 10^4$ the σ–$\bar{\varepsilon}$ curve approaches that of a kink in the vicinity of $\bar{\varepsilon} \approx 0.8$ for a relatively small value of $K_H = 0.01$ while for $K_H = 0.1$ such a kink is completely absent.

The above behavior, described in Fig. 7, can be explained with respect to the relative values of K_E and K_H. We first recognize that, in general, the flexural behavior of a double layer packet, $-L \leqslant X \leqslant L$, is dependent on the ratio $K_H = H/L$, i.e. the

flexural rigidity of the packet increases with increasing values of K_H while as $K_H \to 0$ the packet approaches that of a thin sheet having no flexural stiffness.

With respect to K_E, it is clear in the range $[1, \infty)$, that as K_E decreases, the behavior of the medium approaches that of a homogeneous body. (As shown in Section 3.2, the derived solution for the behavior of the body approaches that of a single isotropic elastic medium as $K_E \to 1$). Consequently, one should expect K_H to have a decreasing influence as K_E decreases. This is reflected in the linear behavior (independent of K_H) for a relatively small value of K_E, e.g. $K_E = 10$.

On the other hand, for increasing values of K_E (e.g. $K_E = 10^4$) the composite behavior of the medium, by definition, assumes increasing importance and one should therefore expect the parameter K_H to have a significant influence on the behavior.

Having recognized that the parameter K_H represents effectively the flexural component of the behavior of the material, for a low value, $K_H = 0.01$, the behavior of the stiffer layer approaches that of a thin sheet (having effectively a very low flexural stiffness). This leads us to an explanation for the kink-like behavior of the $K_E = 10^4$, $K_H = 0.01$ curve in the neighborhood of $\bar{\varepsilon} \approx 0.8$.

We first note that for the initially cosinusoidal template curve under consideration with $\Omega_0 = 30°$, we have from (5.4), $S_L = 1.07874L$ and thus, using (5.5a), $\bar{\varepsilon}_* = 7.874\%$, which is precisely the neighborhood in which this "kink-like" behavior occurs.

To explain this phenomenon further, let us discuss a limiting case. For $K_E \gg 10^4$, the interaction of the stiffer layer with the weaker becomes negligible. Thus (with E_2 fixed and $K_E \to \infty$) the extension of the composite can be asymptotically represented as the extension of a system of separate curvilinear layers. Now, in general, the extension of a curvilinear layer is due to the combination of two different mechanisms: straightening as a result of unbending and axial elongation. If $K_H \to 0$, then the flexural rigidity approaches zero, and hence the response of the layer approaches the behavior of a thin sheet as previously mentioned. It is clear that under tension, the thin sheet first becomes straight (up to $\bar{\varepsilon} = \bar{\varepsilon}_*$) and thereafter it elongates. Thus, since here the two mechanisms occur *sequentially*, a kink appears in the σ–$\bar{\varepsilon}$ curve. For finite K_H, the extension of the rod is governed *simultaneously* by its bending rigidity and by its axial rigidity; thus, no sharp kink is present.

The analogy with the thin sheet can be observed in Figs 8 and 9. We note that the ratio a/A is clearly inversely proportional to the "curviness" of the deformed layer, since $a/A = 0$ defines a straight layer in the deformed state. From Fig. 8, we observe that in the case $K_E = 10^4$ and $K_H = 0.01$, the amplitude initially decreases very rapidly under a very small stress, since owing to the low flexural rigidity, unbending of the layer occurs with little effort. As K_H increases, larger stresses are required to straighten the layer. As in Fig. 7, we again observe in Fig. 8 that the a/A versus σ relation is essentially linear for a relatively low K_E ($K_E = 10$) and is effectively independent of K_H.

Figure 9 shows the behavior of a/A versus $\bar{\varepsilon}$. We observe here that for $K_E = 10$ and 10^2 the relation is quite linear. However, for $K_E = 10^4$, we note that the behavior is nonlinear and changes character in the vicinity of $\bar{\varepsilon} = \bar{\varepsilon}_*$; this is due to the change in the mechanism of the deformation: the initial elongation is due primarily to unbending while the latter is mainly due to the axial elongation. We also show in this figure the

behavior of the composite for which one laminate in the packet is inextensible. It is clear† that in this case (we assume $A/L \ll 1$ and thus $a/L \ll 1$) we have approximately

$$\bar{\varepsilon} = \bar{\varepsilon}_* - Ca^2,$$

where C is a constant. Since $\bar{\varepsilon} = 0$ and $a = A$ in the initial state, we obtain

$$a/A = (1 - \bar{\varepsilon}/\bar{\varepsilon}_*)^{1/2}, \tag{5.7}$$

which is a purely geometrical relation. For $\bar{\varepsilon} \leqslant \bar{\varepsilon}_*$ we observe that the curve corresponding to $K_E = 10^4$ and $K_H = 0.01$ approaches (5.7) asymptotically which reflects the behavior of an inextensible thin sheet.

Figure 10 shows the relation between the stress and the average axial strain, ε_s, defined as

$$\varepsilon_s = s/S - 1, \tag{5.8}$$

where s is the actual arc length determined according to the relation $s = \int_0^{S_L} (\mathbf{r}' \cdot \mathbf{r}')^{1/2} \, dS$. In contrast with the σ–$\bar{\varepsilon}$ curves, the curves in Fig. 10 are linear for all values K_E and K_H. Moreover, the influence of K_H is not significant in these curves.

As previously observed in Fig. 7, the stress and strain curve is "quasi" linear for all values of K_H for relatively small values of K_E, say $K_E \leqslant 10$. This leads us to introduce a normalized macro Young's modulus $\bar{E}$, defined as

$$\bar{E} = \frac{d\sigma/du}{\bar{E}^{(0)}}, \quad \text{where } \bar{E}^{(0)} = \frac{v_1 E_1}{1 - v_1^2} + \frac{v_2 E_2}{1 - v_2^2}. \tag{5.9}$$

Here $\bar{E}^{(0)}$ corresponds to the macro Young's modulus for the straight laminate composite under plane strain. The results are shown in Fig. 11 where we observe a very strong dependence of $\bar{E}$ on both Ω_0 and K_E. We note that, according to its definition, as $K_E \to 1$, $\bar{E} \to 1$.

A comparison of the results obtained by numerical integration with those given by the analytic solution of Section 4 for small initial waviness is shown in Figs 12 and 13.

Figure 12 shows very good agreement between the numerical solution and the analytical approximation (4.42) for $\Omega_0 = 10°$ and $K_E = \{10, 10^2, 10^3, 10^4\}$; $K_H = 0.01$. Since for such Ω_0 the interesting behavior of the σ–$\bar{\varepsilon}$ curves occurs under smaller stresses (than in the case when $\Omega_0 = 30°$), results are given for values $\sigma \in [0, 0.2]$ GPa.

In Section 4 we noted that the relation for a/A, (4.36), is independent of Ω_0. Since

† For an inextensible line we have $\mathbf{r}' \cdot \mathbf{r}' = 1$ or $x'^2 + y'^2 = 1$. Hence $x' = (1 - y'^2)^{1/2} \approx 1 - \frac{1}{2}y'^2$ which, upon integration, yields $l = S_L - 0.5 \int_0^{S_L} y'^2 dS$. Since $S_L - l = (\bar{\varepsilon}_* - \bar{\varepsilon})L$, we have

$$\bar{\varepsilon}_* - \bar{\varepsilon} = \frac{1}{2L} \int_0^{S_L} y'^2 dS.$$

Representing $y(S) = af(S)$, where $f(0) = 1$, we arrive at $\bar{\varepsilon}_* - \bar{\varepsilon} = Ca^2$, where $C = 0.5L^{-1} \int_0^{S_L} f'^2 dS$. If $\int_0^{S_L} f'^2 dS$ does not change during the deformation process or, in particular, if only the amplitude changes but $f(S)$ itself does not change in the process of deformation, then C can be assumed to be a constant and therefore it is not actually necessary to calculate C. This case is approximately valid for the initially cosinusoidal shape considered here but may be incorrect for an arbitrary initial shape.

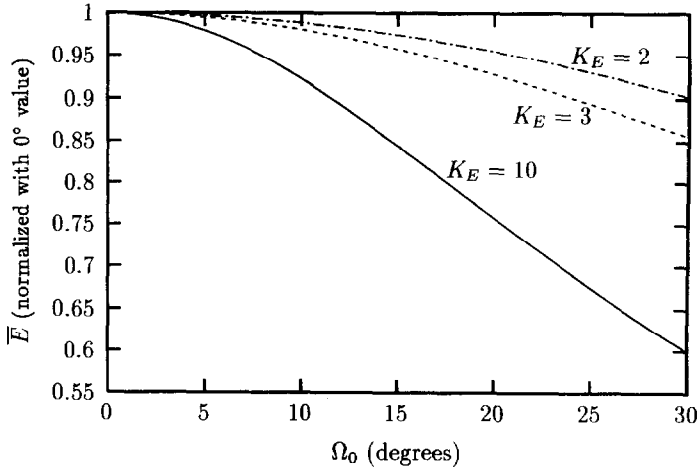

Fig. 11. Effect of Ω_0 on macro Young modulus for different values of $K_E = E_2/E_1$; $v_1 = v_2 = 0.5$, $K_H = 0.05$.

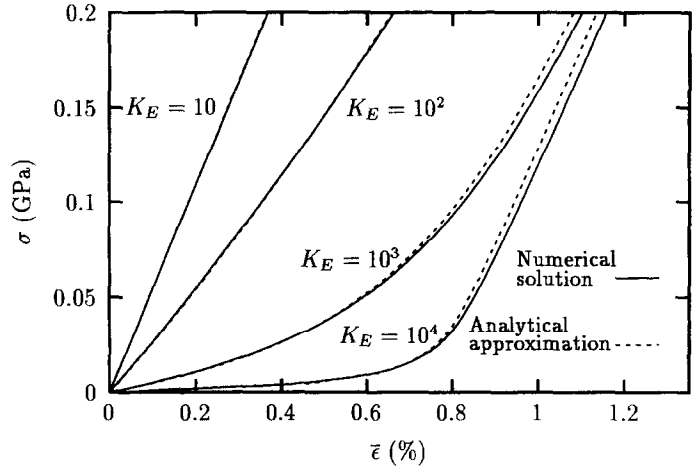

Fig. 12. Comparison between the numerical solution and analytical approximation for $\Omega_0 = 10°$ and typical values of $K_E = E_2/E_1$; $v_1 = v_2 = 0.5$; $K_H = 0.01$.

(4.36) is an approximation which was derived assuming Ω_0 to be small, it is of interest to investigate the influence of Ω_0 on the a/A–σ curves. For $K_H = 0.01$, Fig. 13 shows a comparison between the analytical approximation, which as we have mentioned is independent of Ω_0, and the numerical solution for a relatively large value of Ω_0, $\Omega_0 = 30°$. We observe a slight deviation between the analytical approximation and the numerical solution for $K_E = 10$ and $K_E = 100$ and note that this deviation almost disappears for large values of K_E, e.g. $K_E = 10^3$ and $K_E = 10^4$.

It is of interest to determine the influence of the volume concentration on the behavior. Resulting stress–strain curves, determined from the analytical approximation (4.42), are presented in Fig. 14 for an initially cosinusoidal packet with $\Omega_0 = 10°$, having material properties $E_1 = 0.1$ GPa, $v_1 = 0.25$, $E_2 = 100$ GPa,

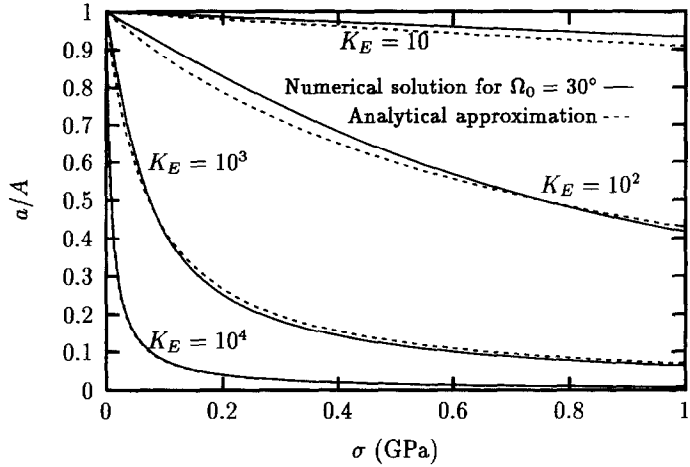

Fig. 13. Comparison between the numerical solution and analytical approximation for $\Omega_0 = 30°$ and typical values of $K_E = E_2/E_1$; $v_1 = v_2 = 0.5$, $K_H = 0.01$.

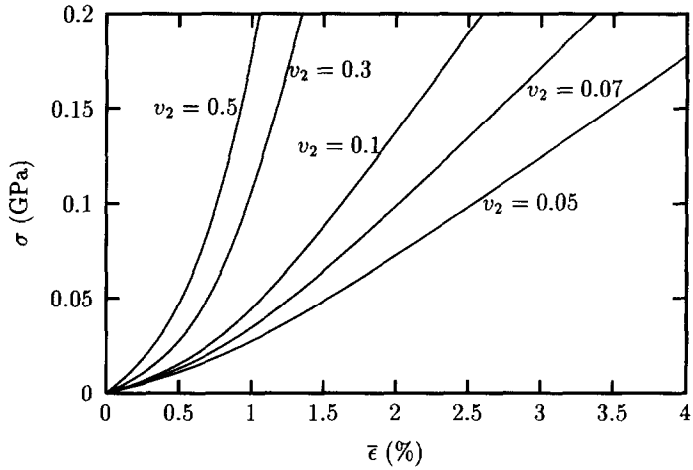

Fig. 14. Effect of volume concentration on stress–(macro) strain curves. Results calculated using analytical approximation; $K_E = 10^3$, $K_H = 0.01$, $\Omega_0 = 10°$, $v_1 = 1 - v_2$.

$v_2 = 0.40$, by a family of curves with $v_2 = \{0.05, 0.07, 0.1, 0.3, 0.5\}$, $v_1 = 1 - v_2$ in the range $\sigma \in [0, 0.2]$ GPa. We observe that initially (say, $v_2 = 0.5$) the curves are clearly nonlinear but rapidly approach linearity (when v_2 decreases). Furthermore, we observe as expected that the composite material becomes significantly stiffer as the volume concentration, v_2, of the stiffer layer increases.

Finally, we compare the results given here with those obtained by Chou and Takahashi (1987). We first observe that the parameter K_H is absent in Chou and Takahashi (1987) as well as in Luo and Chou (1988, 1990). It was implicitly assumed in these works that $K_H \to 0$. (This parameter is also absent in Skoller and Hegemier (1995) where, assuming that $K_H \to 0$, the first term of the asymptotic expansion is

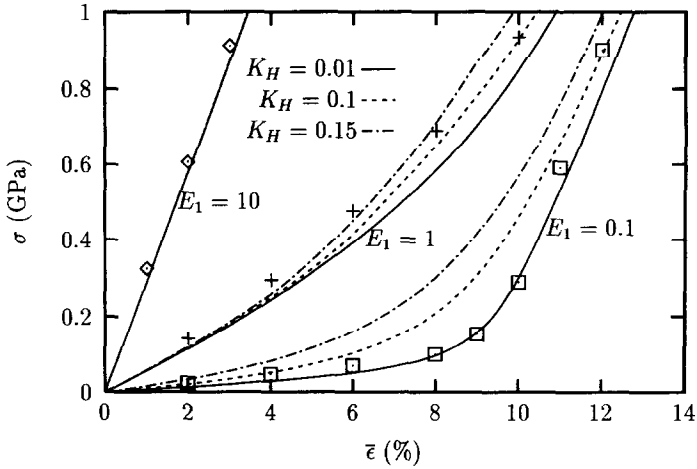

Fig. 15. Comparison between numerical results (shown by lines) and results of Chou and Takahashi (1987) (marked by points) for different values of $K_E = E_2/E_1$ and $K_H = H/L$; $v_1 = v_2 = 0.5$, $\Omega_0 \approx 32°$.

present). Thus, by neglecting the parameter K_H in these works, bending rigidities of the layers were not taken into account.

A comparison between the predicted behavior of our model (shown for different values of $K_H = \{0.01, 0.1, 0.15\}$) and the results of the incremental analysis of Chou and Takahashi (1987) (marked by points†) is presented in Fig. 15. (The same material properties as in Chou and Takahashi (1987) have been used here, namely $E_1 = \{0.1, 1.0, 10\}$ GPa, $v_1 = 0.40$, $E_2 = 72.52$ GPa and $v_2 = 0.22$; volume concentrations $v_1 = v_2 = 0.5$; maximal initial angle $\Omega_0 = \arctan(0.1\pi) \approx 32°$.) For relatively small differences in the material properties of the layers ($E_1 = 10$ GPa, $E_2 = 72.52$ GPa, i.e. for $K_E = 7.25$), the two solutions are in good agreement for all values of K_H. Note that this result is consistent with our analysis of the results of Fig. 7, where it was found that K_H has apparently no influence on the behavior for relatively small K_E. However, in the case of a significant difference in the material properties of the layers ($E_1 = 0.1$ GPa, $E_2 = 72.52$ GPa, i.e. for $K_E = 725.2$), we observe that the results given by Chou and Takahashi (1987) are in good agreement only for small values of K_H, e.g. $K_H = 0.01$; for larger values of K_H, e.g. $K_H = 0.1$ and $K_H = 0.15$, a significant difference exists in the solutions.

From the above analysis, we may conclude that in order to predict properly the behavior for the given problem, one must take the flexural rigidity into account. The laminate model, as presented by Chou and Takahashi (1987) as well as by Luo and Chou (1988 and 1990), whereby flexural rigidity is neglected, will predict correct behavior only for cases where the difference in the material stiffness of the layers is not great ($K_E < 10$) and/or where the relative thickness of the packet $K_H = H/L$ is of the order 0.01.

ACKNOWLEDGEMENT

This research was partially supported by grant No. 94-00349 from the United States–Israel Binational Science Foundation (BSF), Jerusalem, Israel.

† Numerical values are taken from Fig. 7 of this reference.

REFERENCES

Adkins, J. E. (1956) Finite plain deformation of thin elastic sheets reinforced with inextensible cords. *Phil. Trans. R. Soc. Lond.* **A249,** 125–150.

Antman, S. S. (1972) The theory of rods. In *Handbuch der Physik*, Vol VIa/2, ed. C. Truesdell. Springer-Verlag, New York.

Antman, S. S. (1994) *Nonlinear Problems of Elasticity*. Applied Mathematical Sciences, Vol. 107. Springer-Verlag, New York.

Bensoussan, A., Lions, J. L. and Papanicolaou, G. (1978) *Asymptotic Analysis of Periodic Structures*. North-Holland, Amsterdam, New York.

Cherkaev, A. and Slepyan, L. (1995) Waiting element structures and stability under extension. *Int. J. Damage. Mech.* **4**(1), 58–82.

Chou, T. W. and Takahashi, K. (1987) Non-linear elastic behavior of flexible composites. *Composites* **18,** 25–34.

Eliseev, V. V. (1988) The non-linear dynamics of elastic rods. *Prikladnaya Matematika i Mechanika* **52,** 635–641 (in Russian); translated in *Appl. Math. Mech.* **52,** 493–498.

Feltman, R. S. and Santatre, M. H. (1994) Evolution of fibre waviness during the forming of aligned fibre/thermoplastic composites. *Composites Manufacturing* **5,** 203–215.

Fraeijs de Veubeke, B. M. (1979) A Course in Elasticity. In *Applied Mathematical Sciences*, Vol 29. Springer-Verlag, New York.

Little, R. W. (1973) *Elasticity*. Prentice-Hall International, Inc., London.

Luo, S. Y. and Chou, T. W. (1988) Finite deformation and nonlinear elastic behavior of flexible composites. *J. Appl. Mech.* **55,** 149–155.

Luo, S. Y. and Chou, T. W. (1990) Finite deformation of flexible composites. *Proc. R. Soc. Lond.* **A429,** 569–586.

Pipkin, A. C. (1977) Finite deformations in materials reinforced with inextensible cords. In *Finite Elasticity*, ed. R. S. Rivlin, AMD, Vol, 27. The American Society of Mechanical Engineers, New York.

Pipkin, A. C. and Rogers, T. G. (1971) Plane deformation of incompressible fiber-reinforced materials. *J. Appl. Mech.* **38,** 634–640.

Skoller, S. and Hegemier, G. (1995) Homogenisation of plain wave composites using two-scale convergence. *Int. J. Solids. Struct.* **31,** 783–794.

Spencer, A. J. M. (1972) *Deformation of Fibre-Reinforced Materials*. Clarendon Press, Oxford.

APPENDIX A

A.1. *Representation of* $\mathbf{B}_\alpha$ and $(\mathbf{B}_1+\mathbf{B}_2)^{-1}$

We first represent $\mathbf{B}_\alpha$ ($\alpha = 1, 2$) and $(\mathbf{B}_1+\mathbf{B}_2)^{-1}$ to second degree accuracy with respect to the angles of rotation θ_α ($\alpha = 1, 2$). It is convenient to rewrite $\mathbf{B}_\alpha$, (2.36), as

$$\mathbf{B}_\alpha = H\begin{pmatrix} f_\alpha & 0 \\ 0 & g_\alpha \end{pmatrix} \tag{A.1}$$

where, using $H_\alpha = v_\alpha H$, we have

$$f_\alpha = v_\alpha E_\alpha, \quad g_\alpha = v_\alpha G_\alpha, \quad \text{no sum.} \tag{A.2}$$

Thus, owing to (2.34) and (A.1),

$$\mathbf{b}_\alpha = H\begin{pmatrix} f_\alpha \cos^2(\theta_\alpha) + g_\alpha \sin^2(\theta_\alpha) & (f_\alpha - g_\alpha)\cos(\theta_\alpha)\sin(\theta_\alpha) \\ * & g_\alpha \cos^2(\theta_\alpha) + f_\alpha \sin^2(\theta_\alpha) \end{pmatrix}, \text{ no sum.} \tag{A.3}$$

where "*" denotes a component of a symmetrical matrix. With second order accuracy, we obtain

$$\mathbf{b}_\alpha = H\begin{pmatrix} f_\alpha+(g_\alpha-f_\alpha)\theta_\alpha^2 & (f_\alpha-g_\alpha)\theta_\alpha \\ * & g_\alpha+(f_\alpha-g_\alpha)\theta_\alpha^2 \end{pmatrix}, \quad \text{no sum.} \tag{A.4}$$

The inverse matrix, $\mathbf{b}^{-1}=(\mathbf{b}_1+\mathbf{b}_2)^{-1}$, to second degree accuracy, is then

$$\mathbf{b}^{-1} = H^{-1}E^{-1}G^{-1}\begin{pmatrix} G+E^{-1}(GD_2+D_1^2) & -D_1 \\ * & E+G^{-1}(-ED_2+D_1^2) \end{pmatrix}. \tag{A.5}$$

Here we have introduced the notations (note that the subscript D_k means that the term is of order k)

$$E=f_1+f_2, \quad G=g_1+g_2,$$
$$D_1=(f_1-g_1)\theta_1+(f_2-g_2)\theta_2, \quad D_2=(f_1-g_1)\theta_1^2+(f_2-g_2)\theta^2. \tag{A.6}$$

A.2. Representation of $\mathbf{P}(\theta_\alpha)\mathbf{B}_\alpha\mathbf{t}_0$

Let us denote

$$\mathbf{s}_\alpha = \mathbf{b}_\alpha\mathbf{P}_\alpha\mathbf{t}_0, \quad \text{no sum.} \tag{A.7}$$

Since

$$\mathbf{P}_\alpha\mathbf{B}_\alpha\mathbf{t}_0 = H\begin{pmatrix}\cos\theta_\alpha & -\sin\theta_\alpha\\ \sin\theta_\alpha & \cos\theta_\alpha\end{pmatrix}\begin{pmatrix} f_\alpha & 0\\ 0 & g_\alpha\end{pmatrix}\begin{pmatrix}\cos\Omega\\ \sin\Omega\end{pmatrix}, \quad \text{no sum,} \tag{A.8}$$

we have, to second degree accuracy,

$$\mathbf{s}_\alpha = H\begin{pmatrix} f_\alpha-\dfrac{f_\alpha}{2}(\Omega^2+\theta_\alpha^2)-g_\alpha\Omega\theta_\alpha \\ f_\alpha\theta_\alpha+g_\alpha\Omega \end{pmatrix}, \quad \text{no sum.} \tag{A.9}$$

Therefore, we obtain the vector

$$\mathbf{s}=\mathbf{s}_1+\mathbf{s}_2 = H\begin{pmatrix} E-\dfrac{E}{2}\Omega^2-\dfrac{f_1\theta_1^2+f_2\theta_2^2}{2}-(g_1\theta_1+g_2\theta_2)\Omega \\ f_1\theta_1+f_2\theta_2+g\Omega \end{pmatrix}. \tag{A.10}$$

A.3. Calculation of $\mathbf{r}'$

Owing to (3.3) we have

$$\mathbf{r}'=\mathbf{b}^{-1}(F\mathbf{i}+\mathbf{s}). \tag{A.11}$$

We assume ε, introduced via (4.4), to be small; i.e. $|\varepsilon|\ll 1$. Using (A.5), (A.10), and (A.6), we write, to second degree accuracy,

$$\begin{aligned} x' = 1+\varepsilon-\frac{\Omega^2}{2} &-f^{-1}(f_1\theta_1+f_2\theta_2)\Omega \\ &+E^{-1}G^{-1}\left(-\frac{1}{2}f_1g_1+\frac{1}{2}f_1g_2-g_1g_2\right)\theta_1^2 \\ &+E^{-1}G^{-1}\left(-\frac{1}{2}f_2g_2+\frac{1}{2}f_2g_1-g_1g_2\right)\theta_2^2 \\ &+E^{-1}G^{-1}(-f_1g_2-f_2g_1+2g_1g_2)\theta_1\theta_2, \end{aligned} \tag{A.12}$$

$$y' = \Omega + G^{-1}(g_1\theta_1 + g_2\theta_2).$$

Note that we neglect the second order term† εD_1 in the relation for y'.

A.4. Calculation of forces $\mathbf{Q}_\alpha$ *with linear accuracy*

Owing to (2.32), (2.33) and (A.7), the force $\mathbf{Q}_k$ is

$$\mathbf{Q}_\alpha = \mathbf{b}_\alpha[\mathbf{r}' - \mathbf{P}(\theta_\alpha)\mathbf{t}_0] = \mathbf{b}_\alpha\mathbf{r}' - \mathbf{s}_\alpha, \quad \text{no sum.} \tag{A.13}$$

Using representations (A.4), (A.12), and (A.9) we can write

$$\mathbf{b}_\alpha = H\begin{pmatrix} f_\alpha + O_2 & (f_\alpha - g_\alpha)\theta_\alpha \\ * & g_\alpha + O_2 \end{pmatrix}, \quad \mathbf{r}' = \begin{pmatrix} 1 + \varepsilon + O_2 \\ \bar{\theta} + O_2 \end{pmatrix}, \quad \mathbf{s}_\alpha = H\begin{pmatrix} f_\alpha + O_2 \\ f_\alpha\theta O_\alpha + g_\alpha\Omega \end{pmatrix}, \text{–no sum} \tag{A.14}$$

where $\bar{\theta}$ has been defined in (4.3). Here O_N is shorthand for the notation $O([\theta_1, \theta_2, \Omega, \varepsilon], N)$ as defined in Section 4.2. Thus we obtain, with linear accuracy,

$$\mathbf{b}\mathbf{r}' = H\begin{pmatrix} f_\alpha(1+\varepsilon) \\ (f_\alpha - g_\alpha)\theta_\alpha + g_\alpha(\Omega + \bar{\theta}) \end{pmatrix}, \quad \mathbf{s}_\alpha = H\begin{pmatrix} f_\alpha \\ f_\alpha\theta_\alpha + g_\alpha\Omega \end{pmatrix}, \tag{A.15}$$

which gives

$$\mathbf{Q}_1 = H\begin{pmatrix} f_1\varepsilon \\ g^{-1}g_1g_2(\theta_2 - \theta_1) \end{pmatrix}, \quad \mathbf{Q}_2 = H\begin{pmatrix} f_2\varepsilon \\ -g^{-1}g_1g_2(\theta_2 - \theta_1) \end{pmatrix}. \tag{A.16}$$

A.5. Calculation of Λ_{12} *with linear accuracy*

The generalized force factor is

$$\mathbf{F} = v_1\mathbf{Q}_2 - v_2\mathbf{Q}_1 = H\begin{pmatrix} (v_1f_2 - v_2f_1)\varepsilon \\ -g^{-1}g_1g_2(\theta_2 - \theta_1) \end{pmatrix}, \tag{A.17}$$

where we have used $v_1 + v_2 = 1$. Using (3.7), we then have

$$\Lambda_{12} = \mathbf{k}\cdot\mathbf{r}' \times \mathbf{F} = x'F_y - y'F_x = -Hx'g^{-1}g_1g_2(\theta_2 - \theta_1) - Hy'(v_1f_2 - v_2f_1)\varepsilon. \tag{A.18}$$

To obtain linear relations with respect to the angles θ_1, θ_2, and Ω, we substitute $x' = 1 + \varepsilon$ and $y' = \Omega + \bar{\theta}$ and using (4.3) arrive at

$$\Lambda_{12} = -v_1v_2H((1+\varepsilon)G^{-1}G_1G_2(\theta_2 - \theta_1) + (\Omega + \bar{\theta})(E_2 - E_1)\varepsilon). \tag{A.19}$$

A.6. Proof that $\Lambda > 0$

We assume that both G_1 and G_2 are not zeroes ($G_1 > 0$ and $G_2 > 0$). If one of them, say G_1 is zero then, by virtue of (4.9), $\Lambda = v_1^2v_2HE_2\varepsilon$ is clearly positive for any $\varepsilon > 0$ (stretching force).

If both G_1 and G_2 are not zeroes, then G_1G_2 and G are strictly positive. Thus it is clear that, to prove that Λ, defined by (4.9), is positive it is sufficient to show that

$$G_1G_2 + v_1v_2(G_2 - G_1)(E_2 - E_1) \tag{A.20}$$

is non-negative. Substituting $E_\alpha = 2G_\alpha(1 + \nu_\alpha)$ (no sum, $\alpha = 1, 2$) into (A.20), we arrive at

† Since ε is small, $\varepsilon D_1 = \varepsilon[(f_1 - g_1)\theta_1 + (f_2 - g_2)\theta_2)]$ can always be neglected with respect to the $G^{-1}(g_1\theta_1 + g_2\theta_2)$ term. Note that we cannot make a similar simplification in the relation for x'.

$$G_1G_2+2v_1v_2(G_2-G_1)(G_2(1+v_2)-G_1(1+v_1)),$$

which can be represented in the following quadratic form with respect to G_1 and G_2:

$$Q(G_1,G_2)=aG_1^2+bG_2^2+[1-(a-b)]G_1G_2, \tag{A.21}$$

with the coefficients

$$a=2v_1v_2(1+v_1),\ b=2v_1v_2(1+v_2). \tag{A.22}$$

It is easy to show that

$$a,b\in[0,1]. \tag{A.23}$$

To show this we note that since $v_1\geqslant 0$, $v_2\geqslant 0$ and $v_1+v_2=1$, the maximum value of v_1v_2 is 1/4 and is reached at $v_1=v_2=1/2$; thus $v_1v_2\in[0,1/4]$. The Poisson's ratio is in any case positive and no more than 1†. Then we observe that a, b are within the bounds (A.23).

We therefore need only investigate the quadratic form (A.21) under *constraints*

$$G_1\geqslant 0,\quad G_2\geqslant 0. \tag{A.24}$$

Owing to these constraints we cannot use the well-known Sylvester criteria. However, we note that the quadratic form (A.21) can be represented as

$$Q(G_1,G_2)=(\sqrt{a}G_1-\sqrt{b}G_2)^2+[1+2\sqrt{a}\sqrt{b}-(a+b)]G_1G_2$$

or

$$Q(G_1,G_2)=(\sqrt{a}G_1-\sqrt{b}G_2)^2+[1-(\sqrt{a}-\sqrt{b})^2]G_1G_2. \tag{A.25}$$

Since

$$1-(\sqrt{a}-\sqrt{b})^2\geqslant 0\quad \text{for any}\quad a,b\in[0,1], \tag{A.26}$$

we observe that the quadratic form Q under constraints, (A.24), is non-negative determinate. Hence Λ is always positive.

APPENDIX B: CASE OF EQUAL POISSON'S RATIOS

For the case of equal Poisson's ratios, the relations for A_x, A_y, B_x, and K can be simplified. Since the Poisson's ratios in both layers are the same,

$$\frac{G_1}{E_1}=\frac{G_2}{E_2}$$

and, in particular,

$$\frac{G_\alpha}{G}=\frac{E_\alpha}{E},\ (\alpha=1,2)$$

from which

$$\frac{G_2-G_1}{G}=\frac{E_2-E_1}{E}.$$

As a direct consequence of this relation and the relations (4.29) and (4.30) we obtain $A_x=A_y$.

Let us denote the relation of the Young moduli in the layers as

† The "usual" Poisson's ratio $v\in[0,1/2]$, but in the plane problem it is recalculated as $v/(1-v)\in[0,1]$.

$$\gamma = \frac{E_1}{E_2}. \tag{B.1}$$

From (4.29) and (4.30), we then have

$$A_x = A_y \equiv A = \frac{v_1 v_2 (1-\gamma)}{v_2 + v_1 \gamma}. \tag{B.2}$$

Similarly, after some manipulation, we obtain

$$B_x = -\frac{A^2}{2} + \frac{v_1 v_2}{(v_2 + v_1\gamma)^2} v\gamma. \tag{B.3}$$

Thus we can write (4.28) as

$$\frac{\mathrm{d}x}{\mathrm{d}X} = 1 + \varepsilon + \frac{\Omega^2}{2} - \frac{(\Omega + A\omega)^2}{2} + \frac{v_1 v_2}{(v_2 + v_1\gamma)^2} v\gamma\omega^2,$$

$$\frac{\mathrm{d}y}{\mathrm{d}Y} = \Omega + A\omega. \tag{B.4}$$

Finally, we write out the relation for K. From (4.25) we have

$$K = \frac{(1-\gamma)\varepsilon}{v_1 v_2 \dfrac{\pi^2 H^2 (v_2 + v_1\gamma)}{12L^2} + \dfrac{\gamma(1+\varepsilon)}{v_1 + v_2\gamma}\dfrac{G_2}{E_2} + v_1 v_2 \dfrac{(1-\gamma)^2}{v_2 + v_1\gamma}\varepsilon}. \tag{B.5}$$

If Ω is sinusoidal, averaging the relation for $\dfrac{\mathrm{d}x}{\mathrm{d}X}$, (B.4), and using the relation $\omega = -K\Omega$, we arrive at

$$\bar{\varepsilon}(\varepsilon) = \varepsilon + \frac{\Omega_0^2}{4}\left[1 - (1 - AK)^2 + \frac{v_1 v_2}{(v_2 + v_1\gamma)^2} v\gamma K^2\right]. \tag{B.6}$$